Received: 30 July 2024 | Revised: 10 February 2025 | Accepted: 15 February 2025

DOI: 10.1111/joa.14242

Journal of Anatomy | ANATOMICAL SOCIETY WILEY

ORIGINAL ARTICLE

Skull morphology and histology indicate the presence of an unexpected buccal soft tissue structure in dinosaurs

Henry S. Sharpe[1] | Yan-yin Wang[1] | Thomas W. Dudgeon[2,3] | Mark J. Powers[1] | S. Amber Whitebone[4] | Colton C. Coppock[1] | Aaron D. Dyer[2,3] | Corwin Sullivan[1]

[1]Department of Biological Sciences, University of Alberta, Edmonton, Alberta, Canada

[2]Department of Ecology and Evolutionary Biology, University of Toronto, Toronto, Ontario, Canada

[3]Department of Natural History, Royal Ontario Museum, Toronto, Ontario, Canada

[4]Palaeoscience Research Centre, University of New England, Armidale, New South Wales, Australia

Correspondence
Henry S. Sharpe, Department of Biological Sciences, University of Alberta, Edmonton, T6G 2E9, Canada.
Email: sutherland.sharpe@gmail.com

Funding information
Natural Sciences and Engineering Research Council of Canada

Abstract

Unlike mammals, reptiles typically lack large muscles and ligaments that connect the zygoma to the mandible. Dinosaur craniomandibular soft tissue reconstructions, often based on the rationale of extant phylogenetic bracketing, follow this general rule. However, descending flanges from the zygomata of hadrosaurs, heterodontosaurids, and psittacosaurids have been used to argue for a masseter-like muscle in these dinosaur taxa. We examined dinosauriform skulls for osteological indicators of connective tissue entheses on the zygoma and mandible, and subsequently sectioned 10 specimens for histological evidence. Osteological indicators were found on the zygoma in most sampled dinosauriforms, which range from rugosities to large descending processes, and morphologically resemble known muscular and ligamentous entheses. Similarly, rugose features oriented towards the zygoma were found on the mandible in sampled dinosauriforms, many having previously been interpreted as entheses for the adductor mandibulae muscle group. Serial histological sectioning of ceratopsid, hadrosaurid, and tyrannosaurid jugal and surangular rugosities reveals an external cortex rich in collagen fibres, strongly resembling entheseal fibres. Jugal entheseal fibres are usually oriented ventrally towards the surangular, and in hadrosaurids and tyrannosaurids these are parallel to macroscopic striations on the surfaces of the jugal flange. Histological sections of extant chicken buccal regions show similar entheseal fibres in the attachments of the jugomandibular ligament on the jugal and of the adductor musculature on the mandible. We hypothesise a strong connective tissue structure bridging the zygoma and mandible in dinosaurs, termed the 'exoparia'. This structure's size and proximity to the craniomandibular joint would be advantageous in stabilising the mandible relative to the cranium during jaw movement, particularly in dinosaurs thought to process their masticate. A ligamentous or muscular identity for the exoparia cannot be determined with the available data, but the size and shape of the zygomatic entheses in many dinosaurs are more consistent with a muscular attachment. Possible antecedents in non-dinosauriform archosaurs and derivations in modern birds may exist, but the homology of the exoparia is currently unknown. These results highlight the complex soft tissue evolution of dinosaurs and caution against

simplified phylogenetic model-based approaches to tissue reconstruction that ignore contrasting osteological signals.

KEYWORDS
evolution, fossil, myology, paleontology

1 | INTRODUCTION

With few exceptions (e.g. Brown, 1916; Kellner, 1996; Zheng et al., 2021), non-bony connective tissue is not preserved in the dinosaur fossil record. This presents a limitation for studies in areas such as functional morphology and behaviour, which require prior anatomical information on these types of tissues (Witmer, 1995). To inform such studies, dinosaur muscles and ligaments are often reconstructed based on osteological structures that are hypothesised to be homologous with particular entheses in modern animals (Dilkes et al., 2012). Early attempts at this often chose one or more species of extant birds or reptiles as a model for interpreting osteological correlates of dinosaur soft tissues (e.g. Galton, 1969; Lull & Wright, 1942). However, this method of directly copying the musculature of an extant taxon onto an extinct one failed to account for inter- and intraspecific variations and the exact homologies of the soft tissues used (Dilkes et al., 2012), partially stemming from inadequate recognition of these homologies until more recently (Abdala & Diogo, 2010; Holliday & Witmer, 2007; Rowe, 1986). Additionally, terminology often differed for homologous structures between birds, crocodilians and squamates, largely due to different research groups publishing on the connective tissues of different amniote clades (Holliday & Witmer, 2007; Romer, 1923).

Bryant and Russell (1992) and Witmer (1995) later established methods for the application of phylogenetic frameworks to soft tissue reconstructions for extinct taxa. They argued for anatomical inferences to be made using the closest extant outgroups that branched before and after the clade of interest, thus providing a 'bracket' for comparison, which Witmer (1995) standardised as the extant phylogenetic bracket (EPB) approach. Following this method, the closest two outgroups of the extinct taxon of interest are selected; for dinosaurs, these are extant crocodilians and birds. The state of a soft tissue character is assessed in both of these outgroups. If this structure is present in both, its presence is inferred in the extinct taxon. If this tissue is present in only one of the extant outgroups, it is equivocally likely to be present or not within the extinct taxon. If this tissue is absent in both extant outgroups, it is hypothesised to be absent in the extinct taxon. Osteological correlates for these tissues are then sought out where applicable (e.g. a muscle will often leave a visible enthesis on a bone, but a four-chambered heart will not; Witmer, 1995). By its nature, the EPB is unable to support the presence in extinct taxa of novel soft tissue structures that do not occur in their closest extant outgroups (Witmer, 1995).

The EPB has become the standard for soft tissue reconstructions in extinct dinosaurs, particularly for myological reconstructions. These reconstructions hypothesise a large group of mandibular adductors connecting the temporal region to the mandible, a depressor spanning the posterior mandible to the paroccipital process, and a pterygoideus group spanning the posterior mandible to the palate (Figure 1b; Burch, 2014; Dempsey et al., 2023; Fearon & Varricchio, 2016; Holliday, 2009; Jasinoski et al., 2006). However, some attempts have deviated from the EPB approach and instead reconstructed musculature based on osteological structures without a phylogenetic constraint. Sereno (2010) and Sereno et al. (2012) reconstructed an additional jaw muscle beyond those predicted by an EPB approach in *Heterodontosaurus* (Figure 1c) and *Psittacosaurus*. This muscle, termed the *M. adductor mandibulae externus ventralis* (MAMEV) after a similar muscle in extant parrots (Zusi, 1993), was reconstructed as extending from the large jugal flange to the mandible and having a similar topology to a mammalian masseter. Sereno et al.'s (2010) reconstruction of *Psittacosaurus* also included an *M. pseudomasseter* (also after a muscle unique to parrots; Zusi, 1993) connecting the maxilla and dentary anterior to this MAMEV. The inclusion of these muscles was justified by their presence in modern parrots, and the terminology used reflected this (Sereno, 2012; Sereno et al., 2010). This interpretation was challenged in *Psittacosaurus* by Taylor et al. (2017), on the grounds that skull strains in a finite element analysis of a *Psittacosaurus* skull increased when these muscles were present. Studies concerning ornithischian jaw muscles since Sereno et al. (2012) and Sereno et al. (2010) have ignored this interpretation or rejected it based on lack of support in the framework of the EPB, limiting cranial attachments of jaw muscles to the temporal region and palate (Button et al., 2023; Dilkes et al., 2012; Nabavizadeh, 2020b).

In non-avian dinosaurs, the zygomatic region (Figure 1a, composed of the jugal and quadratojugal) shows significant morphological diversity, contrary to the simple rodlike condition in extant birds (Sullivan & Xu, 2017). In particular, flanges and spurs descending ventrally are common (Figure 1c,d; Nabavizadeh, 2020a). The zygomatic region bears a large ventral flange in most known iguanodontians (Horner et al., 2004; Norman, 2004), some heterodontosaurids (Sereno, 2012), at least one stegosaurian (Galton & Upchurch, 2004), some sauropods (Sullivan & Xu, 2017, figure 4 therein; Zaher et al., 2011) and at least one theropod (Lee et al., 2014). Many large theropods possess conspicuous ventral 'cornual processes' in the same location (Sullivan & Xu, 2017). The jugal of pachycephalosaurians is laterally ornamented (Maryańska et al., 2004). Finally, ceratopsians and many thyreophorans hypertrophy the jugal ventrally into a massive process (Dodson et al., 2004). Several of these features have been proposed as entheses in jaw musculature reconstructions,

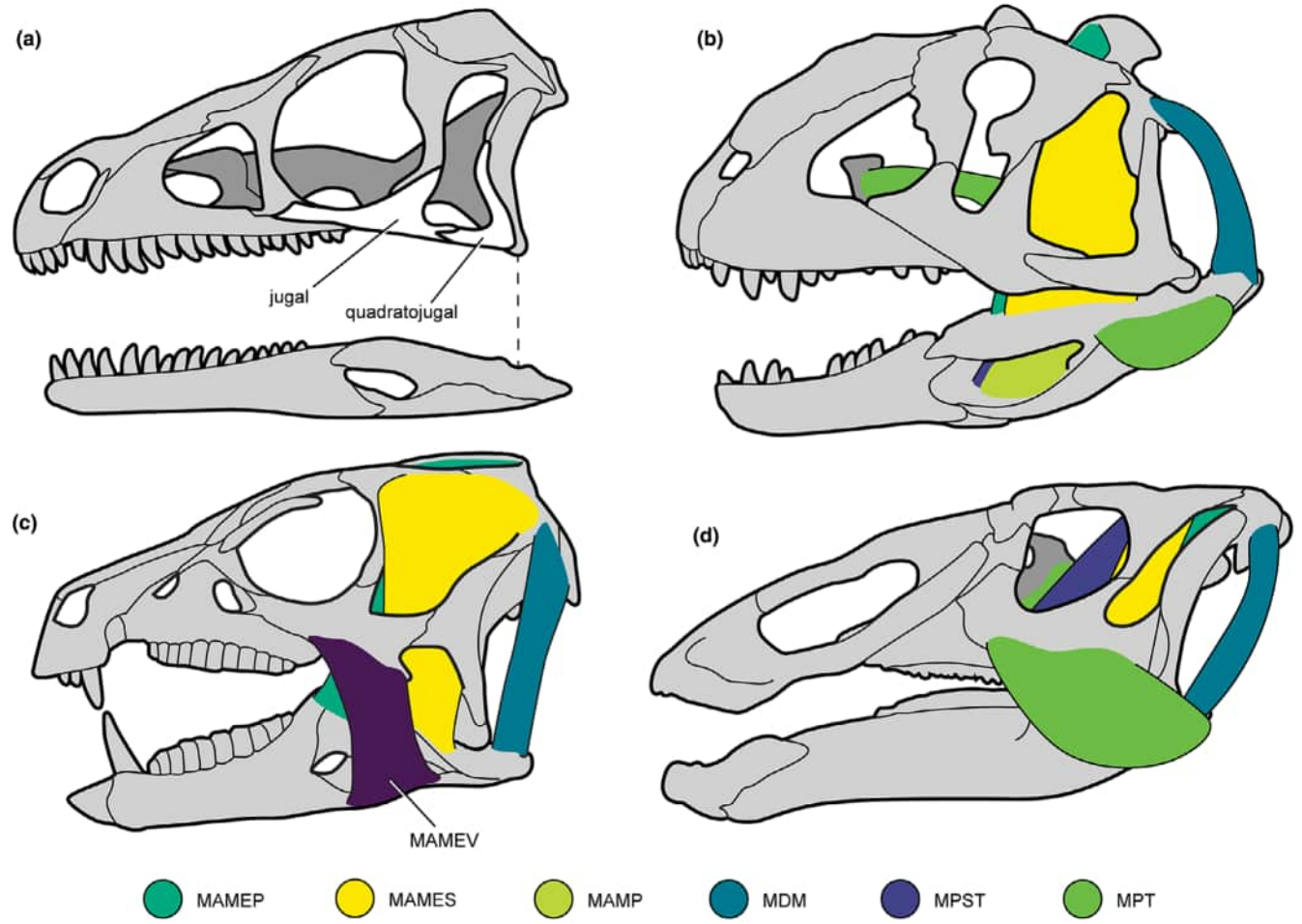

FIGURE 1 Previous myological reconstructions of dinosaur skulls in left lateral view. (a) Skull of the early dinosaur *Eoraptor* (redrawn from Sereno et al., 2012) showing the location and composition of the zygoma; (b) skull of the theropod *Majungasaurus* showing the conservative jaw muscle model predicted by EPB (redrawn from Holliday, 2009); (c) skull of ornithischian *Heterodontosaurus* showing hypothesised MAMEV (redrawn from Sereno, 2012); (d) skull of hadrosaurid *Edmontosaurus* showing a hypothesised extension of *M. pterygoideus* onto the jugal flange (redrawn from Holliday, 2009). Illustrations not to scale. MAMEP, *M. adductor mandibulae externus profundus*; MAMES, *m. adductor mandibulae externus superficialis*; MAMP, *M. adductor mandibulae profundus*; MDM, *M. depressor mandibulae*; MPST, *M. pseudotemporalis*; MPT, *M. pterygoideus*.

including in Sereno (2010)'s and Sereno et al. (2012)'s reconstruction of the MAMEV (Figure 1c), as well as conservative reconstructions using muscles predicted using the EPB (Figure 1d; Holliday, 2009; Lautenschlager, 2013; Lee et al., 2014). Like those proposed by Sereno et al. (2010) and Sereno et al. (2012), these reconstructions have since been considered unlikely (Sullivan & Xu, 2017).

Despite these morphologically diverse conditions in extinct dinosaurs, extant archosaurs have largely unmodified zygomata (Figure 2). This is likely a consequence of these taxa lacking any major muscular attachments on the ventrolateral zygoma, instead concentrating their adductor musculature into the temporal region (Holliday & Witmer, 2007). However, there are some tissues that connect the zygoma to the mandible in these extant groups. In crocodilians, the *m. adductor mandibulae externus superficialis* (MAMES) cranial attachment includes part of the anteromedial surface of the quadratojugal (Figure 2b; Holliday & Witmer, 2007), although in crocodilians, the quadratojugal is largely excluded from the zygoma. In birds, no muscles insert on the jugal or quadratojugal (the MAMES inserts on the squamosal and quadrate instead; Holliday & Witmer, 2007), but two ligaments (*ligamentum jugomandibulare partes laterale et mediale*) connect the posterior jugal–quadratojugal bar to the mandible in opposing directions (Figure 2d). Crocodilians also have two ligaments (the lateral and medial collateral ligaments) proximal to the craniomandibular joint, but the medial collateral ligament is medial to this joint (Figure 2c; Saber & Hassanin, 2014), whereas in birds, the medial jugomandibular ligament is lateral to the craniomandibular joint (Figure 2d; Hassan, 2012). In birds, a third ligament, the ligamentum postorbitale, connects the postorbital to the mandible in this region (Figure 2d; Hassan, 2012). Whether these ligaments may be homologous in birds and crocodilians has never been investigated. Reconstruction of a connective tissue that connects the zygoma and mandible in non-avian dinosaurs would therefore require a Level II or III inference under the EPB (Witmer, 1995), depending on how this question of homology is resolved.

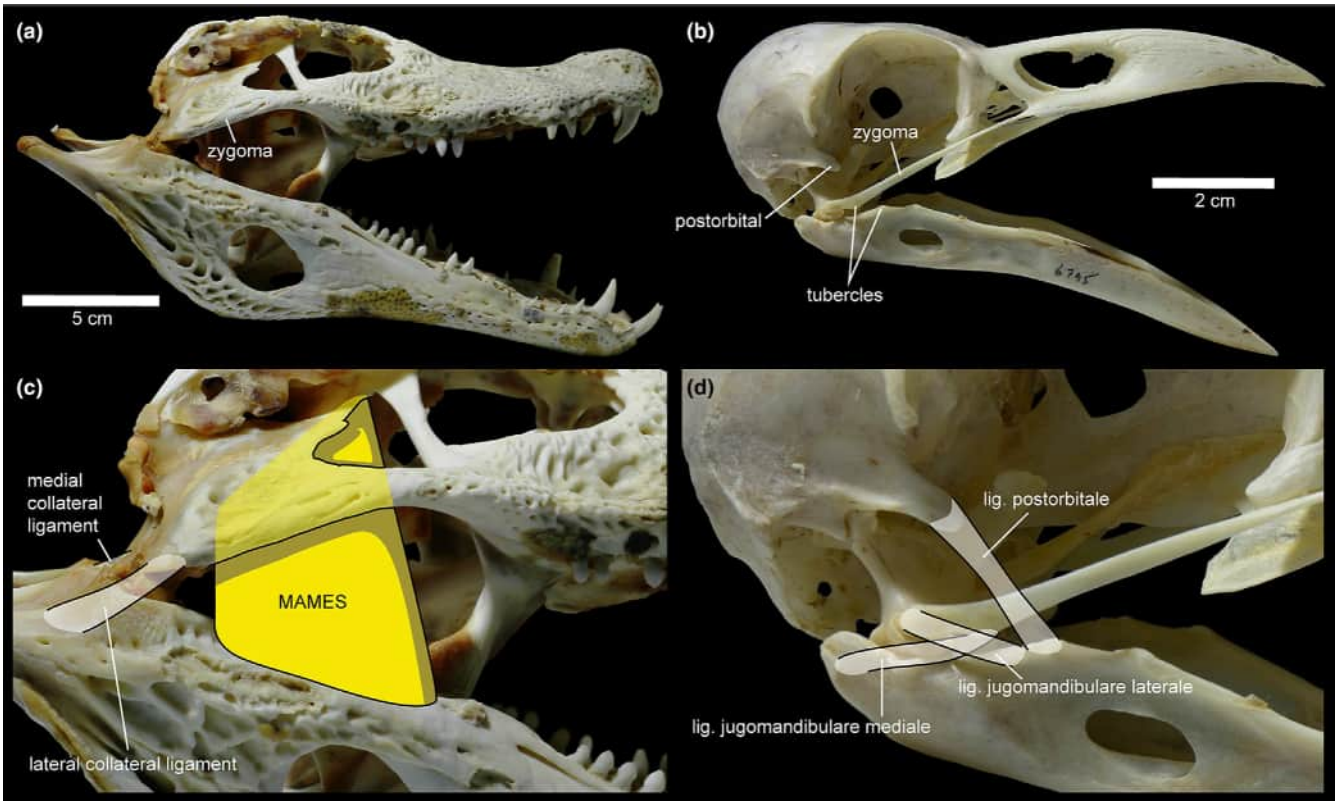

FIGURE 2 Connective tissues in the cheek regions of living crocodilians and birds in right lateral view. (a) Skull of *Caiman* sp. UAMZ uncatalogued, (b) skull of *Corvus corax* UAMZ 6795, (c) enlargement of (a) showing tissues reconstructed from Holliday and Witmer (2007) and Saber and Hassanin (2014), and (d) enlargement of (b) showing tissues reconstructed from Hassan (2012).

While identifying osteological entheses based on external morphology can yield uncertain results (Bryant & Seymour, 1990; Witmer, 1995), histology may be able to provide clarity. Tissues that attach to bone, such as periosteum, muscles, tendons, ligaments, cartilage and dermal structures, may insert collagen fibres into bones that can be recognised in histological slides (Hieronymus, 2006; Jones & Boyde, 1974; Scheyer et al., 2007; Sharpey et al., 1867; Whitebone et al., 2021). The orientation of these fibres can further reflect the orientation at which the soft tissue contacted the bone (Hieronymus, 2006; Whitebone et al., 2021). Here we investigate the plausibility of a soft tissue structure connecting the zygoma to the mandible in dinosaurs. We utilise two approaches: first, a survey of external osteological morphology to identify potential zygomatic entheses and complementary potential mandibular entheses, and second, a histological analysis of these sites to examine intrinsic evidence for entheseal identity.

2 | METHODS

2.1 | Surface morphology

Representative specimens from across Dinosauria (here used inclusively to encompass ornithischians, sauropods and theropods, as well as two groups, Herrerasauridae and Silesauridae, that have been argued to represent early branching dinosaurs; Colbert, 1970; Ferigolo & Langer, 2007) were surveyed, either in person, through computed tomography (CT) or surface scans, or (as a last resort) via photographs. Data obtained as raw CT scans were segmented in Dragonfly v. 2022.1.0.1409. Scans were visualised in Autodesk Maya v. 2024 and MeshLab v. 2022.02. Zygomata and posterior mandibles were examined for possible entheses oriented towards each other. Criteria for identifying possible entheses were the presence of large flanges or processes, striated or rugose external bone textures, ridges or depressions along the oral margin, and ventral bowing of the zygomatic body. For each structure, a search was made in the literature to determine whether a possible cause for said osteological feature had been proposed.

2.2 | Modern histology

Histological sections were made from the head of a *Gallus gallus* (UAMZ unnumbered) that was presumably skeletally mature, being at least 5 years old. These sections were used to examine entheses on and adjacent to the zygoma, which were then used as an extant frame of reference for interpreting thin sections made from sampled fossil taxa. To locate the region of interest on the head, the right side of *G. gallus* (UAMZ unnumbered) was dissected to expose the majority of the zygoma and its surrounding soft tissues. The left side was not dissected before being processed for sections.

The specimen was placed in 10% neutral buffered formalin (prepared using Fisher formaldehyde F79-1) for 2 days to fix the tissues and then placed in Cal-Ex solution (Fisher Scientific CS510-1D, 5.5% hydrochloric acid and 0.12% disodium EDTA dihydrate, pH 2.0) for 30 days of decalcification. On a weekly basis, the level of decalcification was examined on the bones by a manual pressure test using a pair of forceps, followed by replacement of Cal-Ex solutions to maintain an effective process of decalcification. The decalcified specimen was then trimmed into several rostrocaudal blocks using a sharp razor blade. All specimen blocks were fixed again in 10% neutral buffered formalin for 48 h and were subsequently placed in a 50% ethanol solution for 1–3 h. The specimens were then processed overnight in a Leica TP 1020 tissue processor using Program 2. After Program 2 was completed, the specimens were embedded in paraffin wax using a Tissue-Tek II embedding machine. The embedded specimens were placed on ice for at least 20 min before being sectioned at a thickness of 5–7 μm using Leica 2025 BioCut rotary microtome. Serial sections were made in transverse planes from the caudalmost aspect of the maxilla to the quadratomandibular joint. Selected sections from regions of interest were mounted on frosted glass slides (Fisherbrand™ Premium Frosted Microscope Slides) and dried at 37°C in an oven. As targeted tissues were ligaments, all sections were stained using Masson's trichrome technique. Some of the sections were stained with an old batch of Aniline Blue and the others with a brand new one, which likely introduced colour artifacts. Identifications of tissues were based primarily on their morphology. Images of histological sections were captured using a Nikon DS-FI3 camera mounted on a Nikon Eclipse E600 POL microscope and Nikon NIS Elements (v. 4.60) imaging software. Cross-polarised light and a lambda filter were used to visualise entheseal fibres.

The term 'Sharpey's fibres' is broadly used to refer to collagen fibres passing from an external position through the entire periosteum and inserting into the osseous tissues (e.g. Petermann & Sander, 2013; Simmons et al., 1993). This nomenclature is problematic, as W. Sharpey was unaware that these structures had been previously described by at least one other author until after his name had been attached to them by other authors, at which point he attempted to reject his priority (Sharpey, in Schäfer 1878). Additionally, this broad definition is inclusive of fibres anchoring connective tissues to entheses (e.g. Petermann & Sander, 2013), as well as those anchoring the periosteum (e.g. Aaron, 2012) and is often specifically used to describe the attachment and microstructure of the periodontal ligament (e.g. LeBlanc et al., 2017); only the first of these is relevant to this study. We therefore refer to collagen fibres anchoring connective tissues to entheses as 'entheseal fibres' to reflect a restricted anatomical rather than broad patronymic terminology.

2.3 | Paleohistology

Once possible entheses were identified, this hypothesis was tested by histological examination for collagen fibres resembling entheseal fibres from extant samples. Bones from three phylogenetically disparate dinosaur clades were sectioned: hadrosaurids, ceratopsids and tyrannosaurids. Each clade is known from relatively abundant remains in the dinosaur-rich strata of Alberta, Canada. Multiple examples of each element were sectioned when possible. To preserve morphological data, each specimen was either digitised using Metascan v. 2.9 or traditionally moulded in silicone and cast in gypsum cement prior to histological sectioning.

Specimens were embedded in Castolite AC polyester resin, from which air bubbles were removed using a vacuum chamber. Once the resin hardened, the specimens were histologically sectioned using a Buehler Isomet 1000 saw. Cut specimens were ground with 400- and 600-grit silicon carbide, as were glass slides; the specimens were then mounted to the glass slides using cyanoacrylate. The mounted specimens were cut 0.7 mm from the slide on the same saw, after which the cut slide was ground using a Hillcrest grinder, and then further using 400-, 600- and 1000-grit silicon carbide until a suitable thinness was reached.

Images of histological sections were captured using a Nikon DS-FI3 camera mounted on a Nikon Eclipse E600 POL microscope and Nikon NIS Elements (v. 4.60) imaging software. Cross-polarised light and a lambda filter were used to visualise histological features. Large image captures were taken for each sample, following the bone immediately beneath the periosteal surface across the area of interest. Entheseal fibre orientation was manually recorded over these large image captures using the brush tool in Adobe Photoshop CC 2024; this annotated image file was then brought into Adobe Illustrator CC 2024, and larger arrows (for better visibility in the finished figures) were drawn to show general fibre orientation.

The 3D orientation of each extrinsic fibre can be represented by a unit vector with three components: x, y and z. As perpendicular section plane records two of the three direction ($x+y$, $x+z$, or $y+z$) vectors for each fibre, only two sections of different planes were required to determine the orientation of the fibres in the 3D space. Sections were made along two semi-perpendicular planes for each specimen; these planes of section often followed, but were not restricted to, the anatomical planes (coronal, sagittal, transverse), and oftentimes, multiple serial sections were made along the same plane. Once captured, these sections were plotted on a representative surface-scanned skull of each sampled group and the extrinsic fibres were mapped in the 3D space (Figure 3). We are unaware of an existing term for (or indeed, existing examples of) this process, and so term this technique Three-dimensional HistoLogical Enthesis Entry-angle Prediction (THLEEP). If the fibres on the zygoma and mandible were oriented towards each other, a connective tissue was considered likely to be present.

2.3.1 | Institutional abbreviations

AMNH FARB, American Museum of Natural History, New York City, New York, United States of America; BMNHC, Beijing Museum of Natural History, Beijing, China; BP, Evolutionary Studies Institute, University of the Witwatersrand, Johannesburg,

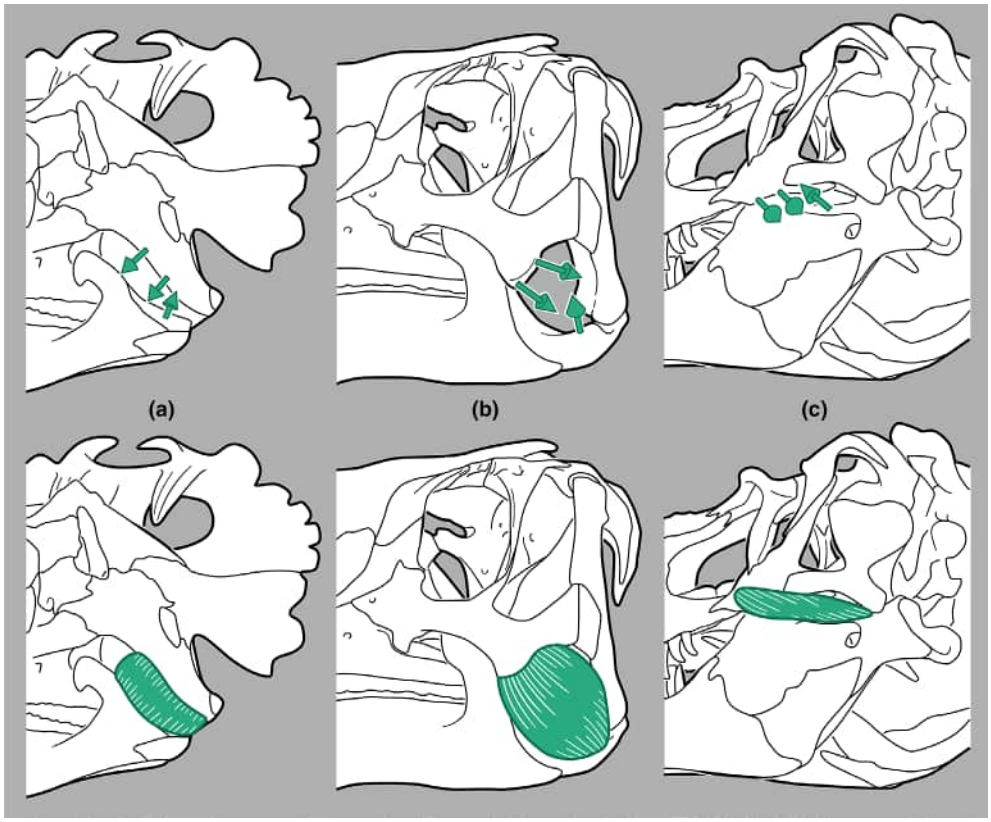

FIGURE 3 Reconstruction of the exoparia via THLEEP in (a) ceratopsids (using *Centrosaurus apertus*, illustrated from UALVP 16248 in left anterolateral oblique view), (b) hadrosaurids (using *Brachylophosaurus canadensis*, illustrated from CMN 8893 in left anterolateral oblique view), and (c) tyrannosaurids (using Tyrannosauridae sp., illustrated from UALVP 52981 in left posterolateral oblique view). Illustrations not to scale.

South Africa; CAPPA/UFSM 0009, Centro de Apoio à Pesquisa Paleontológica da Quarta Colônia/Universidade Federal de Santa Maria, Santa Maria, Rio Grande do Sul, Brazil; CEUM, College of Eastern Utah Prehistoric Museum, Price, Utah; CM, Carnegie Museum of Natural History, Pittsburgh, Pennsylvania, United States of America; CMC, Cincinnati Museum Center, Cincinnati, Ohio, United States of America; CMN, Canadian Museum of Nature, Ottawa, Ontario, Canada; DINO, Dinosaur National Monument, Jensen, Utah, United States of America; FMNH, Field Museum of Natural History, Chicago, Illinois, United States of America; IRSNB, Institut royal des Sciences naturelles de Belgique, Brussels, Belgium; IVPP, Institute of Vertebrate Paleontology and Paleoanthropology, Beijing, China; LP, Institut d'Estudis Ilerdencs, Lleida, Spain; MNHN LES, Muséum national d'histoire naturelle, Paris, France; MPC-D, Paleontological institute, Mongolian Academy of Sciences, Box-46/650, Ulaanbaatar, 15,160, Mongolia; MZSP-Pv, Museu de Zoologia da Universidade de São Paulo, São Paulo, Brazil; NCSM, North Carolina Museum of Natural Sciences, Raleigh, North Carolina, United States of America; PKUP, Peking University Paleontological Collections, Beijing, China; PVSJ, Museo de Ciencias Naturales, Universidad Nacional de San Juan, San Juan, Argentina; ROM, Royal Ontario Museum, Toronto, Ontario, Canada; SAM-K Iziko South African Museum, Cape Town, South Africa; TMP, Royal Tyrrell Museum of Palaeontology, Drumheller, Alberta, Canada; UALVP, University of Alberta Laboratory for Vertebrate Paleontology, Edmonton, Alberta, Canada; UAMZ, University of Alberta Museum of Zoology, Edmonton, Alberta, Canada; YPM, Yale Peabody Museum, New Haven, Connecticut, United States of America; ZDM, Zigong Dinosaur Museum, Zigong, Sichuan, China.

3 | RESULTS

3.1 | Summary of results

External osteological signals that indicate entheseal attachments on the zygomata of dinosaurs are morphologically consistent across many non-avian dinosaurs and early birds. In several of these cases (hadrosaurids, heterodontosaurids, some sauropods), the zygoma is significantly modified by a large descending flange, resembling the condition in certain mammals in which the masseteric attachment on the zygomatic has been elaborated into a large descending flange to accommodate certain masticatory modes (Ercoli et al., 2023; Meinertz, 1944; Naples, 1985; Pereira et al., 2020). Rugosities and crests of the posterior mandible are also visible, towards which the external textures from the zygoma orient. Histological sections of ceratopsids, hadrosaurids and tyrannosaurids reveal similar entheseal fibres to those associated with muscle attachments in modern birds (Figure 4), and in each

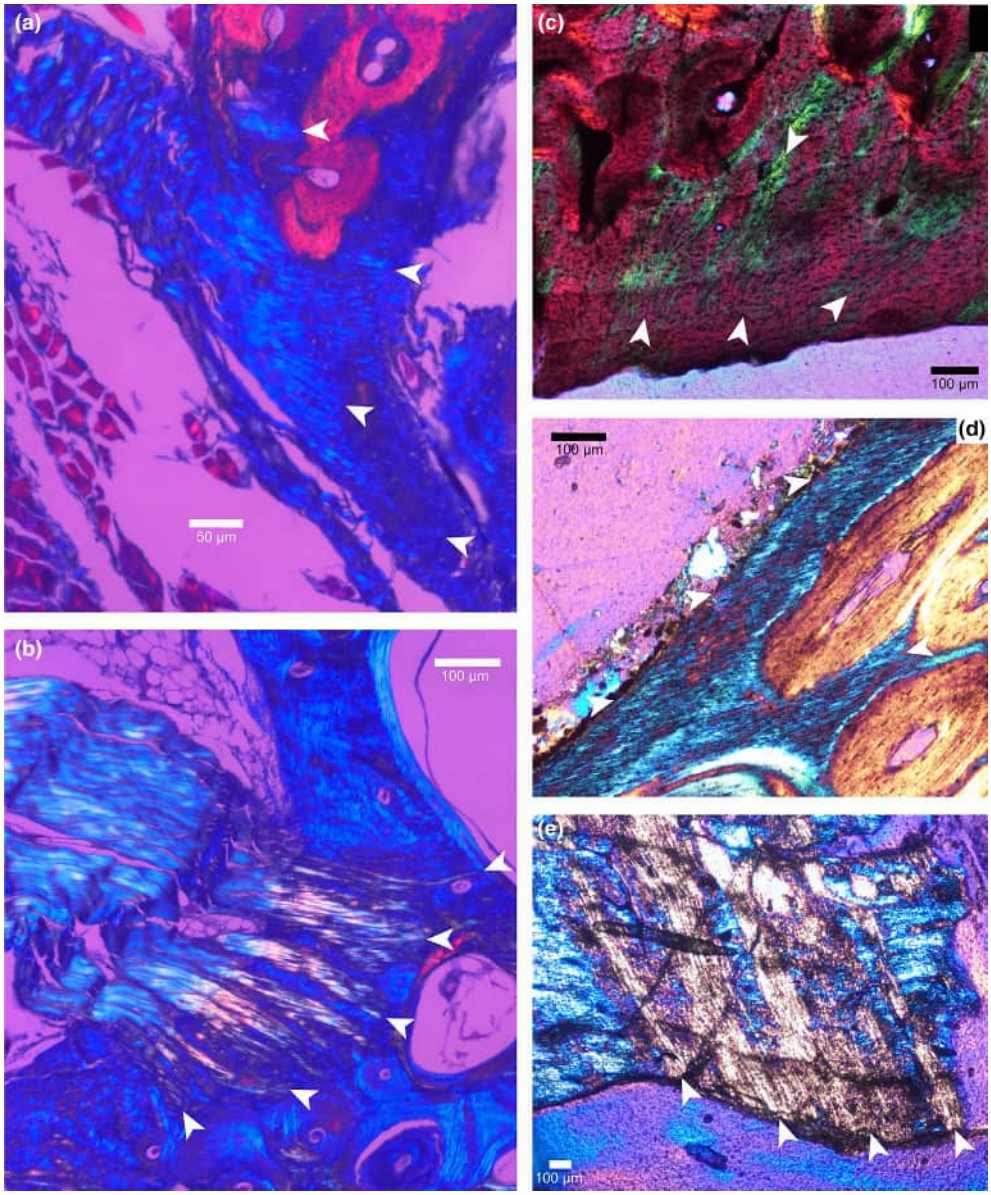

FIGURE 4 Comparison of extant chicken entheseal histology (a, b) to dinosaur entheseal histology (c, d). (a) Transverse/subtransverse thin section at the middle part of mandible, showing tendinous attachment; (b) transverse/subtransverse thin section adjacent to quadromandibular joint, showing attachment site of medial jugomendibular ligament at medial condyle of articular; (c) subcoronal section of ceratopsian jugal TMP 1992.036.0929; (d) transverse/subtransverse section of hadrosaurid jugal TMP 1986.078.0005; (e) parasagittal section of tyrannosaurid jugal TMP 2000.012.0011. Arrows indicate entheseal fibres.

case, THLEEP recovers zygomatic fibres orienting towards the mandible and mandibular fibres orienting towards the zygoma (Figure 3). We therefore hypothesise the existence of a connective tissue, either a muscle or ligament, bridging the zygoma and posterior mandible in dinosaur-line archosaurs. Given the lack of an obvious homologue in modern archosaurs, as well as the current lack of concrete data on the nature (muscle vs. ligament) of this tissue, we provide the anatomical name 'exoparia'. This derives from the Ancient Greek words 'exo-' (prefix, 'outer') and 'pareia' or 'paria' (noun, 'cheek') in reference to its anatomical position in dinosaurs as the most external known major connective tissue body deep to the skin in the buccal region of the head.

3.2 | External osteology

3.2.1 | Herrerasauridae

Herrerasaurids have been proposed as early branching non-theropod dinosaurs (e.g. Novas et al., 2021), early-branching theropods (e.g. Sues et al., 2011), and non-dinosaurian dinosauromorphs (Baron & Williams, 2018), and will be discussed separately here for organisational purposes. Taxa within Herrerasauridae (Figure 5) demonstrate a jugal flange morphology typical among several theropod groups (e.g. Allosauroidea) with a weakly formed ventral projection that is restricted to the ventral margin of the jugal. This type of small ventral

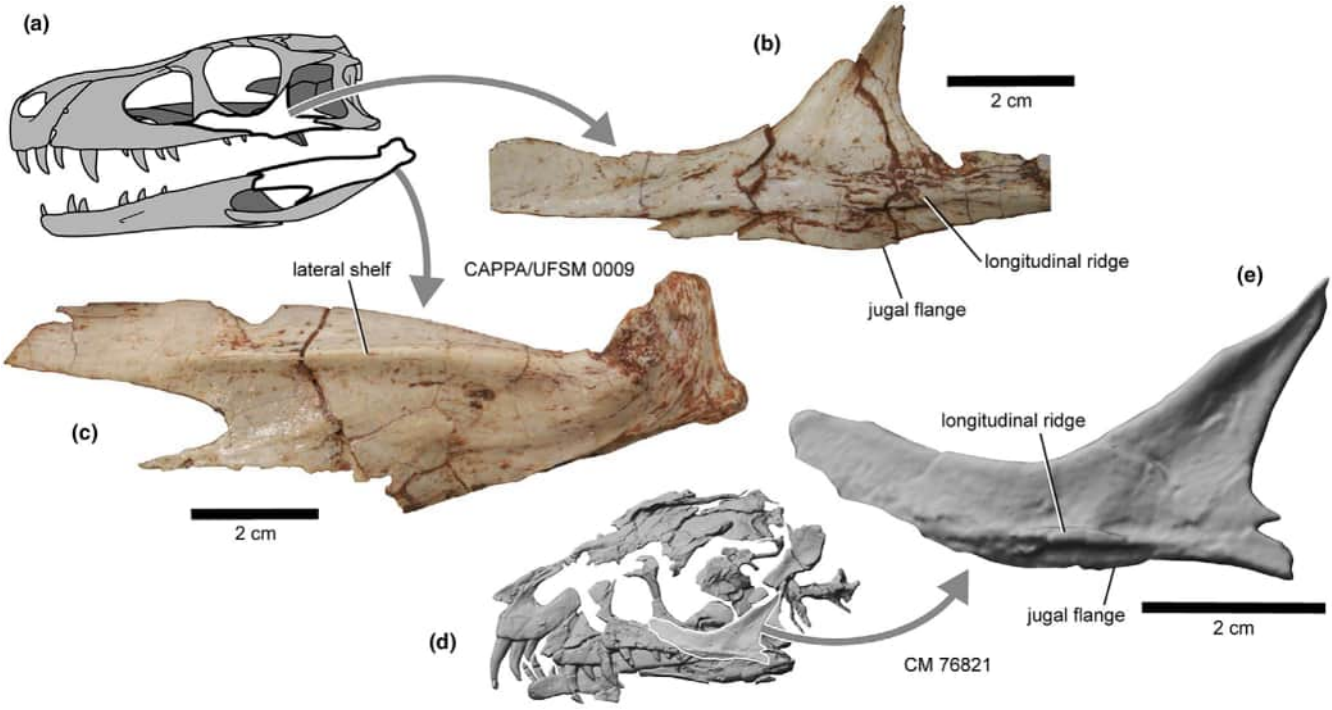

FIGURE 5 Zygomatic and posterior mandibular morphology of representative herrerasaurids in left lateral view. (a) Skull of *Gnathovorax cabreirai* (drawn from Pacheco et al., 2019a, 2019b); (b) right jugal of *G. cabreirai*, mirrored; (c) right surangular of *G. cabreirai*; mirrored (d, e) CT scan of (d) skull and (e) left jugal of *Daemonosaurus chauliodus*.

jugal flange is present, dorsally bordered by a longitudinal ridge on the lateral surface of the jugal, in *Daemonosaurus chauliodus* (Figure 5d,e), *Gnathovorax cabreirai* (Figure 5a–c) and *Herrerasaurus ischigualastensis* (Sereno & Novas, 1994). In *H. ischigualastensis*, the jugal flange originates ventral to the midpoint of the orbit and extends posteriorly to the posterior margin of the quadratojugal contact surface on the jugal. In *G. cabreirai*, the less developed jugal flange originates at the anterior margin of the postorbital process and abruptly terminates in line with the posterior margin of the postorbital process (Figure 5b). The flange is small and rounded in *D. chauliodus* and is located more anteriorly than in *G. cabreirai* and *H. ischigualastensis* (Figure 5e).

Herrerasaurids possess an anteroposteriorly elongate shelf along the dorsal margin of the surangular. In both *G. cabreirai* (Figure 5) and *H. ischigualastensis*, the surangular shelf spans from the region dorsal to the mandibular fenestra posteriorly to the articular contact. The lateral expression of the surangular shelf is most prominent in the posterior region of the shelf, whereas the anterior half is a weakly formed, sub-rounded ridge.

3.2.2 | Silesauridae

Silesaurids have been proposed as early branching ornithischians in some analyses (e.g. Ferigolo & Langer, 2007; Müller & Garcia, 2020) but as non-dinosaurian dinosauriforms in others (Nesbitt, 2009), and will be discussed separately here for organisational purposes. In *Lewisuchus admixtus* and *Silesaurus opolensis*, a longitudinal ridge is present along the lateral surface of the jugal (de Buffrénil et al., 2010; Sullivan & Xu, 2017, figure 2 therein), strongly resembling the herrerasaurid condition. The posterior part of the mandible is not well known in silesaurids, but an anteroposteriorly long surangular shelf was illustrated by Dzik (2003).

3.2.3 | Early branching Ornithischia

In *Lesothosaurus diagnosticus* (MNHN LES 17), there is a small, triangular ventral projection on the jugal ventral to the postorbital process. In many heterodontosaurids, there is a large, rectangular posteroventral flange on the jugal (Sereno, 2012). The jugal flange of *Heterodontosaurus tucki* (TMP 2006.000.0041, cast of SAM-K 1332) is particularly well developed and is bordered proximally by a small, round, laterally projecting boss. This flange has previously been argued to represent an attachment for an additional 'MAMEV' muscle (Sereno, 2012; Figure 1c).

A small bump is present on the surangular anterolateral to the quadrate glenoid in *L. diagnosticus* (MNHN LES 17). A small surangular flange is present in *H. tucki* (Sereno, 2012); the long axis of the jugal flange points almost precisely to the surangular flange in this taxon (Figure 1c).

3.2.4 | Thyreophora

The zygoma of *Scelidosaurus harrisonii* has a posteroventral flange that is predominantly situated on the lateral surface of the quadratojugal

and is dorsally bordered by an anteroposteriorly oriented ridge (Norman, 2020). The zygoma of *Emausaurus ernsti* preserves a similar ridge, but the ventral flange of the zygoma is smaller and predominantly contributed by the jugal (Haubold, 1990). The lateral ridge on both taxa is topologically similar to that in herrerasaurids, silesaurids and early branching sauropodomorphs, but no equivalent feature is visible in more derived thyreophorans. The zygoma is unmodified in most stegosaurians, but in *Stegosaurus* sp. the jugal bears a posteroventrally directed flange (Galton & Upchurch, 2004), reminiscent of the condition in iguanodontians. In ankylosaurians, the zygoma flares out ventrolaterally and the lateral surface of the ventral apex bears a large osteoderm (Vickaryous et al., 2004). The majority of the zygoma, including the osteoderm-bearing ventrolateral flange, is formed by the quadratojugal (Vickaryous et al., 2004). The jugal is reduced and bears a longitudinal ventral eminence that fades into the quadratojugal ventrolateral flange posteriorly (Vickaryous et al., 2004). In *Edmontonia rugosidens* (UALVP 55668, Figure 6b) and *Ankylosaurus magniventris* (UALVP 54722, cast of AMNH FR 5214), this eminence takes the form of a slightly ventrally convex ridge, and in UALVP 55668, the bone surface along the ventral surface of this ridge is rugose. In *Gastonia burgei* (UALVP 54755, cast of CEUM 1307), this eminence is more mediolaterally inflated and better described as a rugosity.

In early branching thyreophorans, there is a distinct dorsally projecting ridge running anteroposteriorly along the posterior half of the surangular (Haubold, 1990; Norman, 2020), the anterior half of which resembles the surangular shelf of theropods. In *Euoplocephalus tutus* (Figure 6c), this surangular ridge is present and forms the lateral border of the adductor fossa anteriorly, but posteriorly it does not, being separated laterally from the quadrate glenoid. This ridge appears identical to the more distinct flange in early branching thyreophorans but lacks the distinct anterior ridge that resembles the theropod condition. This flange is located posterolateral to the presumed attachment area for the adductor musculature (Holliday, 2009). In stegosaurians and early branching thyreophorans, a similar ridge appears to be present (Galton & Upchurch, 2004). This ridge occupies the same position as the surangular flange of other ornithischians, but the posterior half is posterodorsally oriented as in ceratopsians rather than laterally projecting as in ornithopods.

3.2.5 | Thescelosauridae

The zygoma of *Thescelosaurus neglectus* (Figure 6e) bears a ventrally short but anteroposteriorly long ventral flange. This flange is covered by posteroventrally oriented striations and is medially emarginate relative to the lateral surface of the rest of the zygoma (Boyd, 2014). A striate posterolateral jugal boss is present on the jugal of *Orodromeus makelai* (Scheetz, 1999).

The posterior mandible of *T. neglectus* lacks an obvious surangular flange resembling that of other ornithischians, but instead has a large, anterodorsally oriented process at the same locus (Figure 6f; see also Boyd, 2014) that points directly to the jugal flange when the mandible is articulated (Figure 6d). The striations on the jugal flange point towards this process, whose dorsal surface is inflated and rugose. A smaller version of this process is present in *O. makelai* (Scheetz, 1999).

3.2.6 | Ceratopsia

The zygomata of ceratopsians became modified through the course of their evolution due to increasing ventral displacement of the craniomandibular joint (Dodson et al., 2004). The zygoma of *Yinlong downsi* is relatively unmodified, aside from being rugose and having an anterolaterally oriented eminence (Han et al., 2015). In *Psittacosaurus* spp., the jugal forms a large laterally projecting process ('horn') that has been proposed as a 'MAMEV' enthesis (Sereno et al., 2010). In Ceratopsidae (e.g. *Centrosaurus apertus* Figure 6g, *Chasmosaurus* sp. UALVP 40, *Styracosaurus albertensis* UALVP 55900), the jugal protrusion is more ventrally oriented and confluent with the reduced quadratojugal (Figure 6h). The ventrolaterally projecting main body of the ceratopsid jugal bears a ventrolateral epijugal ossification. In many ceratopsid specimens, the anteroventral edge of the ventrolateral ala is a rugose ridge. The rugose surface texture of this ridge continues onto the anteromedial surface of the jugal; posterior to this, the medial surface becomes smooth (excepting the quadratojugal contact). The posterior edge and ventromedial surface of the jugal contact the quadratojugal, which is similarly rugose along the external posterior surface and bears a low obliquely oriented crest.

The surangular of *Y. downsi* bears a prominent lateral tubercle on the surangular, anteroventral to the quadrate glenoid (Han et al., 2015). In ceratopsids, the posterior part of the mandible bears a large anteroposteriorly oriented flange along the posterior dorsolateral margin of the surangular (Figure 6i). The posterior end of this flange is continuous with a dorsally concave arcuate ridge that spans the surangular and angular. Together, these features create a large, rugose plateau on the lateral surface of the posterior part of the mandible.

3.2.7 | Pachycephalosauria

Pachycephalosaurian (sensu Madzia et al., 2021) jugals are posteroventrally expanded and possess rugose ornamentations across the lateral surface (Maryańska et al., 2004; Figure 6j). Large spike-like nodes are present at the posteroventral corner of the jugal in Pachycephalosaurini (Evans et al., 2013; Goodwin & Evans, 2016). The non-pachycephalosaurid pachycephalosaurian *Wannanosaurus yansiensis* appears to possess a straight ventral margin of the jugal (see figure 6 in Butler & Zhao, 2009). In the pachycephalosaurid *Stegoceras validum* (UALVP 2), the ventral margin of the jugal is strongly concave ventral to the anterior portion of the orbit, although the posterior part of the ventral margin is typically illustrated with a slight convexity (see Maryańska et al., 2004; Sues et al., 1987). Pachycephalosaurine jugals possess a moderately well-developed

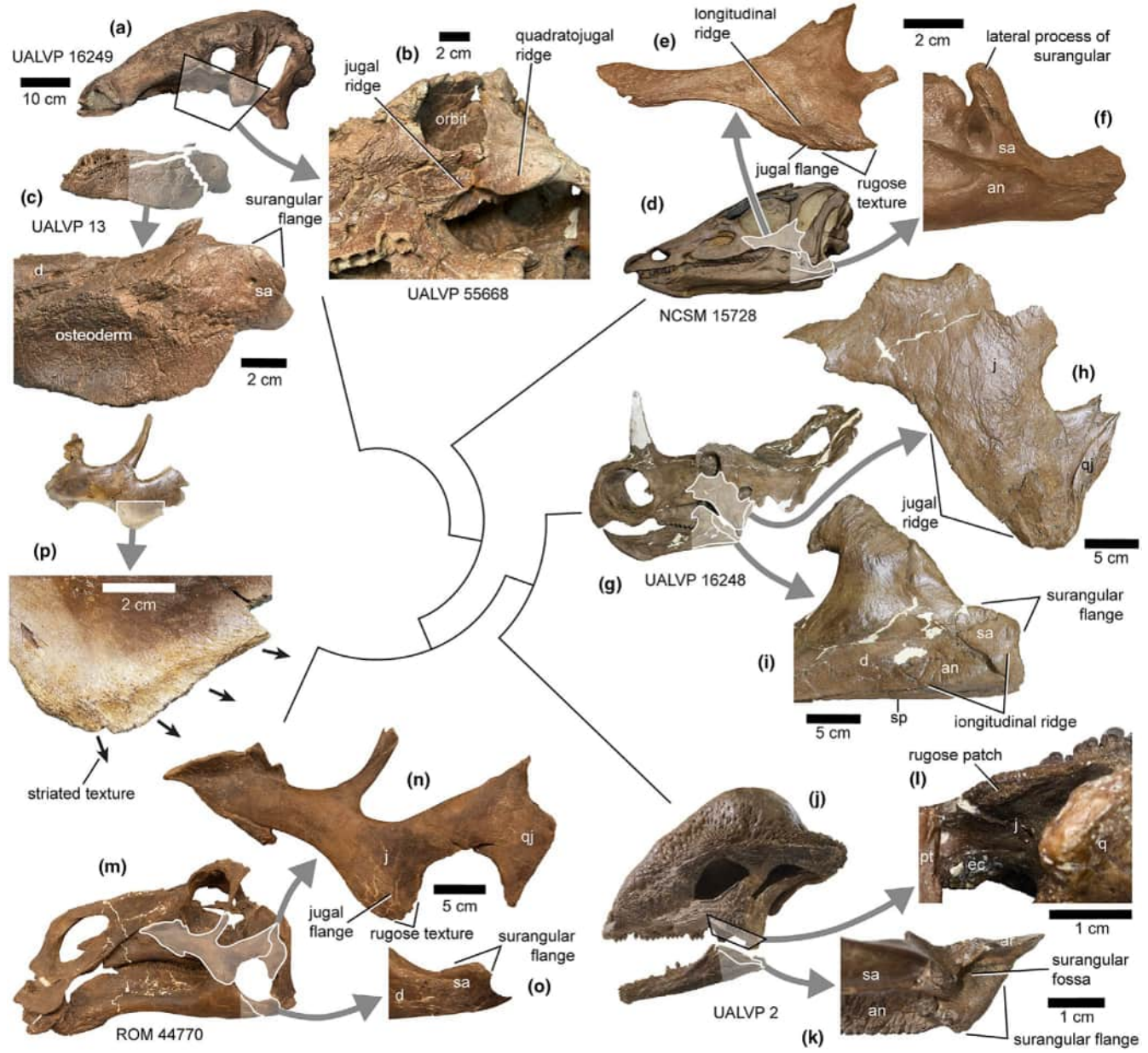

FIGURE 6 Zygomatic and posterior mandibular morphology of representative ornithischians, all in left lateral view unless otherwise stated. (a–c) Thyreophora; (a) *Edmontonia rugosidens*, (b) close-up of *E. rugosidens* cranium in ventral oblique view, and (c) full view and enlargement of posterior mandible of *Euoplocephalus tutus* (mirrored). (d–f) *Thescelosaurus neglectus* (mirrored); (g–i) *Centrosaurus apertus* (mirrored); (j–l) *Stegoceras validum*; (m–o) *Maiasaura peeblesorum* (mirrored); (p) full view and close-up of hadrosaurid jugal UALVP 54667. An, angular; d, dentary; j, jugal; qj, quadratojugal; sa, surangular; sp, splenial.

convex flange along the posteroventral margin, although the flange is relatively poorly developed in *Homalocephale calathocercos* (Bakker et al., 2006; Goodwin & Evans, 2016; Maryańska & Osmólska, 1974). The ventromedial borders of ROM 53671 (*Pachycephalosaurus wyomingensis*) and UALVP 2 show raised, vascularised patches (Figure 6l). Other vascularised regions include the quadradojugal contact and the orbital margin. These patches are oval in shape, well separated from any sutural surface and topologically similar to jugal rugosities in other dinosaurs.

Postdentary bones are only known from a handful of specimens and are often incompletely described (Maryańska & Osmólska, 1974; Perle et al., 1982). The surangular of *S. validum* possesses a deep, anteroposteriorly narrow, dorsally oriented fossa immediately posterolateral to the articular surface for the quadrate and posteromedial to the enlarged surangular/angular mandibular boss (Figure 6k).

3.2.8 | Ornithopoda

Members of this clade typically possess an expanded jugal with a ventral flange; the quadratojugal, by contrast, is reduced. Although the craniomandibular joint tended to shift ventrally over the course

of ornithopod evolution, as in Ceratopsia, this did not significantly affect the zygoma, as this transition occured by ventral extension of the quadrate alone. The relative size of the jugal flange tends to increase with body size and phylogenetic proximity to hadrosauridae, being small in *Zalmoxes* (Weishampel et al., 2003), larger in *Iguanodon* (IRSNB R 55) and largest in hadrosaurids (e.g. *Maiasaura peeblesorum*, Figure 6m,n; *Edmontosaurus regalis* CMN 2288; *Hypacrosaurus altispinus* ROM 702). Similarly, the flange migrates anteriorly from a location ventral to the quadrate contact in early branching members to a 'free' (not immediately ventral to the quadrate contact) morphology in hadrosaurids (Wu et al., 2010). In hadrosaurids, large-bodied derived ornithopods, these trends culminate in a large, variably rugose flange that projects conspicuously in the buccal region of the skull (Figure 6m,p). Posteroventrally oriented striations are common along the lateral surface of the jugal flange in early branching (Weishampel et al., 2003) and derived (e.g. *E. regalis*, UALVP 60425; Figure 6p) ornithopods, leading several authors (Norman, 1986; Tsogtbaatar et al., 2019; Weishampel et al., 2003) to speculate on the jugal flange being an attachment site for cheek tissues. These striations are not uniform within species, for instance, being visible on only some of the Bernissart quarry *Iguanodon* specimens. In some hadrosaurids, the striations on the lateral surface are concentrated on the sulcate posteroventral margin of the flange (similar to *T. neglectus*). In hadrosaurids, rugosities and striations are more abundant on the medial surface of the jugal flange than on the lateral surface; medial textures are unreported in other ornithopods. In some hadrosaurids (e.g. *M. peeblesorum* ROM 44770, Figure 6n), small spurs oriented parallel to these striations line the posteroventral edge of the jugal flange. The ornithopod jugal flange and/or its texturing are invariably oriented towards the region of the surangular flange in articulated skulls.

The surangular flange is more morphologically conservative than the jugal flange within Ornithopoda. In taxa we have examined, the former is a small, typically triangular, dorsolaterally projecting process, located anterolateral to the quadrate glenoid on the surangular (Figure 6o). It is typically relatively larger in larger-bodied taxa (e.g. *Iguanodon*, hadrosaurids). In *Iguanodon*, it is dorsally rounded instead of triangular. It is rugose in all examined specimens, including on the anterodorsal margin (which faces the jugal flange). The flange is robust in hadrosaurids, which has likely contributed to the surangular (and in particular, the region bearing this flange) being one of the most commonly recovered hadrosaurid cranial elements in North American Campanian and Maastrichtian fluvial deposits.

3.2.9 | Sauropodomorpha

The zygomata of early branching sauropodomorphs resemble those of herrerasaurids, silesaurids and early branching thyreophorans in possessing a weak ventral jugal flange that is bordered dorsally by an anteroposteriorly elongate ridge (Figure 7a,b,d,e). This condition is readily visible in some taxa (e.g. *Euraptor lunensis*, PVSJ 512 (Sullivan & Xu, 2017); *Lufengosaurus huenei*, Figure 7d,e; *Ngwevu intloko*, Figure 7a,b), but in others (e.g. *Massospondylus carinatus*, BP/1/4376, BP/1/5241), the flange and ridge are less clearly defined. Within derived sauropods, the jugal is reduced and excluded from the ventral margin of the zygoma by the quadratojugal, which becomes the main component of the zygoma (Figure 7h; Sullivan & Xu, 2017). In the relatively early branching sauropod *Shunosaurus lii* (ZDM T 5403), the jugal is still the predominant bone in the zygoma and bears a large descending ventral flange (Figure 7f,g). In the brachiosaurid *Europasaurus holgeri* (Marpmann et al., 2014), the diplodocid *Apatosaurus* sp. (CMC VP 7180) and the titanosaur *Tapuiasaurus macedoi* (MZSP-Pv 807), the jugal is reduced and largely replaced by the quadratojugal, which shows a large descending ventral flange in the exact same location as the jugal flange in *S. lii* (Figure 7i,j). The quadratojugal flange of sauropods tends to be angled anteroventrally when present (Figure 7g,j), unlike the posteroventrally oriented jugal flange of heterodontosaurids and iguanodontians. In many other sauropod skulls, no such flange is present, but the zygoma is sometimes ventrally bowed in the same region (Wilson & Sereno, 1998, figures 6–8 therein).

The surangulars of *N. intloko* (BP/1/4779) and *M. carinatus* (BP/1/4376) are mostly unornamented, with the exception of a low anteroposterior ridge on the lateral surface ventral to the craniomandibular joint and a lateral eminence dorsal to the mandibular fenestra (Figure 7c). The latter feature is situated immediately ventral to the jugal flange when the jaw is closed (Figure 7a).

3.2.10 | Non-tetanuran theropods

Many coelophysoids show a longitudinal ridge along the lateral surface of the jugal (Bristowe & Raath, 2004; Bugos & McDavid, 2024; Ezcurra, 2007; Rowe, 1989). This ridge is nearly identical to those seen in herrerasaurids, silesaurids, early branching thyreophorans and early branching sauropodomorphs. In abelisaurids such as *Majungasaurus crenatissimus* (Figure 8a–c), the posterior part of the jugal is strongly bowed ventrally. The ventral bowing reaches its apex posterior to the postorbital process. The ventral margin of the jugal is mediolaterally widest at the apex of the bowed region. While the subdermal facial texture of *M. crenatissimus* is typically rugose, the ventral margin of the jugal shows numerous posteroventrally oriented tubercles that are morphologically distinct from the texture on the rest of this bone (Figure 8b).

Both coelophysoids (Rowe, 1989) and abelisaurids (FMNH PR 2100, Figure 8c) have a surangular shelf that is laterally prominent in the vicinity of the craniomandibular joint but recedes anteriorly, closely resembling the shelf of herrerasaurids.

3.2.11 | Allosauroidea

Allosauroid jugals show variation in the morphology of the ventral margin (Carpenter, 2010; Chure & Loewen, 2020; Madsen, 1976). *Allosaurus fragilis* (Figure 8e) and *Acrocanthosaurus atokensis* (Eddy

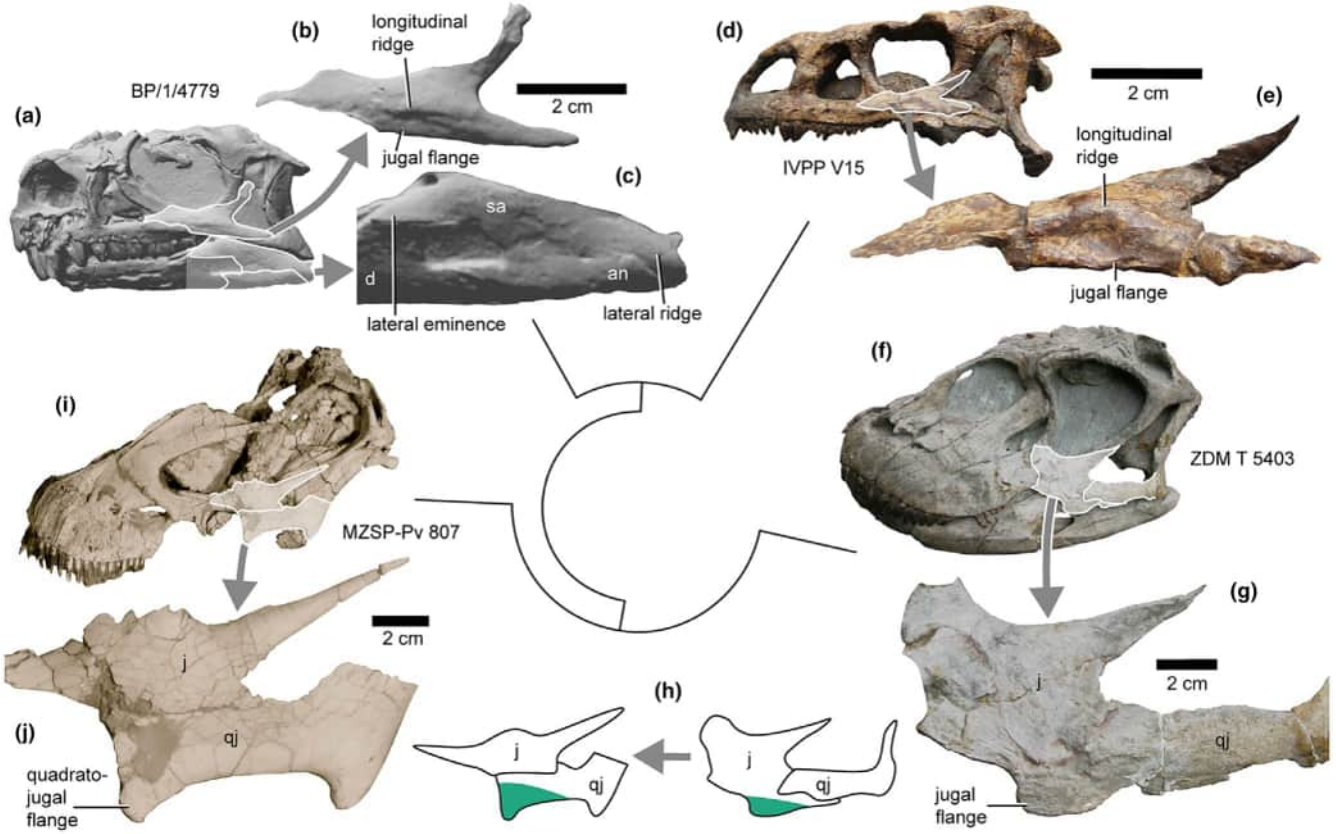

FIGURE 7 Zygomatic and posterior mandibular morphology of representative sauropods in left lateral view. (a–c) *Ngwevu intloko*; (d, e) *Lufengosaurus hueni*; (f, g) *Shunosaurus lii*; (h) transition of zygomatic flange from jugal to quadratojugal in early branching (right) and derived (right) sauropods; (i, j) *Tapuiasaurus macedoi*, photo courtesy of Jeff Wilson Mantilla. An, angular; j, jugal; qj, quadratojugal; sa, surangular.

& Clarke, 2011) have a strong ventral bowing over the entire length of the jugal and lack a distinct ventral flange. However, the anterior portion of the ventral border, posterior to the maxillary contact, is narrowed and covered in striated bone texture directed posteroventrally. This is similar to the condition in *Mapusaurus roseae*, and all three possess a lateral ridge dorsal to the striated area, somewhat resembling herrerasaurids, silesaurids, early branching sauropodomorphs and thyreophorans. In *Carcharodontosaurus saharicus* (Sereno et al., 1996), *Meraxes gigas* (Canale et al., 2022; Canale pers. comm.) and *Tyrannotitan chubutensis*, there is a distinct and mediolaterally thick ventral flange between the maxillary contact and the ventral quadratojugal process. The ventral quadratojugal process has a strong posterodorsal deflection, similar to other allosauroids (Carpenter, 2010; Eddy & Clarke, 2011). There are well-developed posteroventrally oriented ridges along the medial and lateral surfaces of the ventral flange in *M. gigas* and *T. chubutensis*, dorsally bordered by a well-developed anteroposterior ridge on the lateral surface. The ventral flange in *C. saharicus*, *M. gigas* and *T. chubutensis* is most similar to that of herrerasaurids, except for being much more prominent than in the latter. All carcharodontosaurids observed show some variation of the narrowed, striated feature dorsally bordered by a lateral ridge between the maxillary and quadratojugal contacts. The large ventral bowing of the ventral edge of the jugal, including the ventral quadratojugal process, is generally observed in *Allosaurus* spp. (Chure & Loewen, 2020; Figure 8e), similar to *Acr. atokensis* (Eddy & Clarke, 2011). However, considerable variation is observed within and between *Allosaurus* species (Carpenter, 2010; Chure & Loewen, 2020). The bowing of the ventral jugal margin in *Allosaurus* spp. ranges from strong, as in *Acr. atokensis*, to a nearly straight ventral margin oriented anterodorsally between the maxilla and quadratojugal contacts.

The surangular of allosauroids has a prominent lateral shelf, resembling that of other theropods and herrerasaurids, located closely posteroventral to the ventralmost portion of the arching jugal when the mandible is articulated (Eddy & Clarke, 2011; Chure & Loewen, 2020; Figure 8f). The surangular shelf of *Acr. atokensis* shows a slight dorsal upturn anteriorly, whereas some *Allosaurus* specimens have a shelf only posteriorly, beneath the quadratojugal process (Figure 8f).

3.2.12 | Tyrannosauroidea

Within Tyrannosauroidea, the morphology of the jugal flange (alternatively called the cornual process or jugal horn; Carr et al., 2017) varies from a minute ventral projection, typically found in early branching tyrannosauroids, to a larger and more anteriorly situated

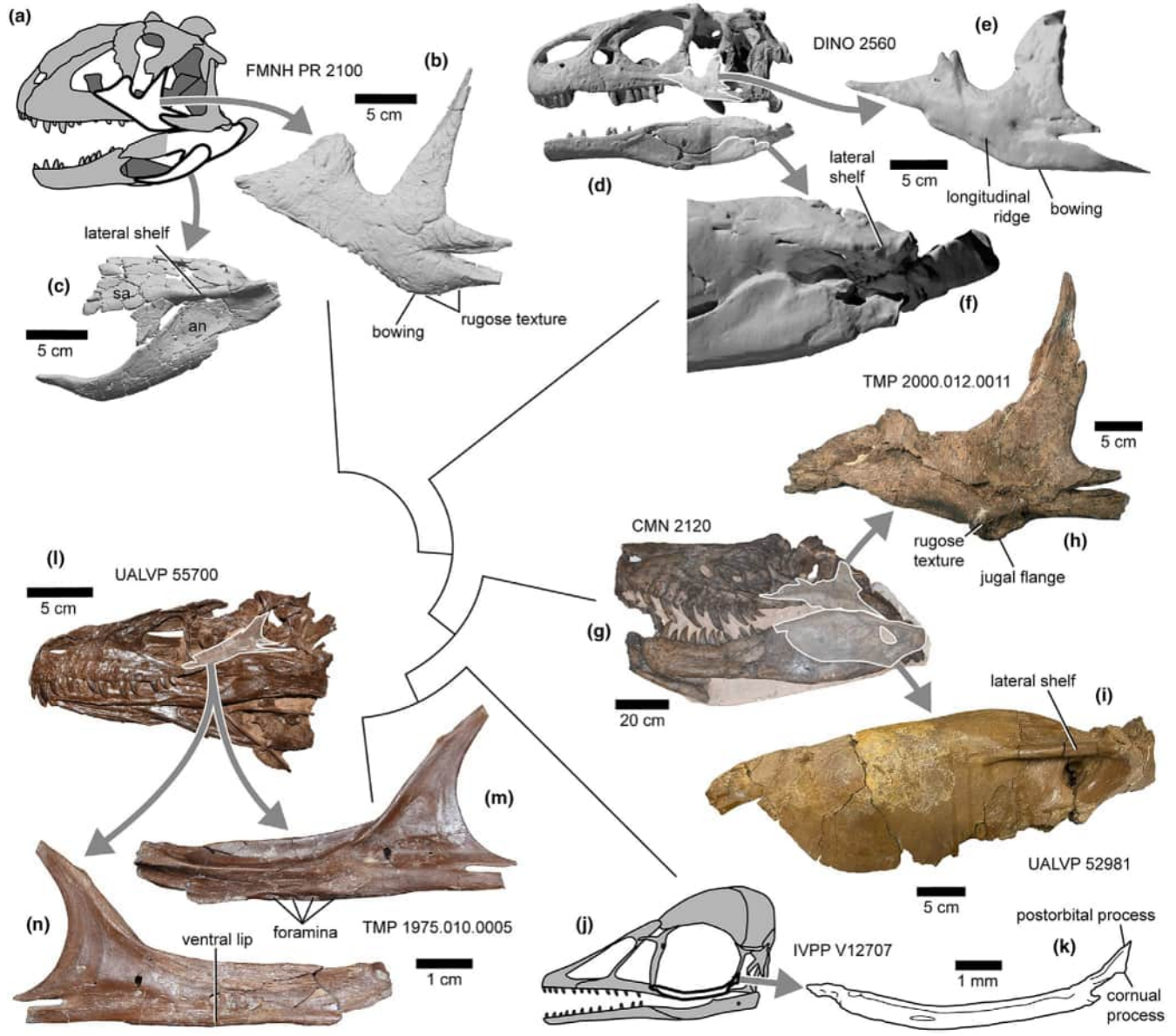

FIGURE 8 Zygomatic and posterior mandibular morphology of representative theropods in left lateral view. (a–c) *Majungasaurus crenatissimus*, (a) drawn from Sampson and Witmer (2007) and (b, c) mirrored; (d–f) *Allosaurus fragilis*; (g, h) *Gorgosaurus libratus*; (i) Tyrannosauridae sp.; (j, k) IVPP V12707 drawn from Wang et al. (2021) and (l–n) *Saurornitholestes langstoni* (mirrored).

ventral projection in derived tyrannosaurids. Proceratosaurids are commonly recovered at the base of Tyrannosauroidea (Brusatte & Carr, 2016) and often display a small and rugose jugal flange posteroventral to the orbit (Rauhut et al., 2010). Proceratosaurids, such as *Proceratosaurus bradleyi* and *Guanlong wucaii*, also possess an anteroposteriorly elongate ridge along the lateroventral margin of the jugal that extends from the anterior margin to the jugal flange. This is similar to the condition noted in herrerasaurids and allosauroids. The proceratosaurid *Yutyrannus huali* possesses a condition more commonly seen in derived tyrannosaurids, with a large and thickened jugal flange positioned ventral to the orbit (Xu et al., 2012; Brusatte & Carr, 2016), and lacks a well-defined jugal ridge. However, the development of this feature may be a result of the large size of the specimen, as most other proceratosaurids are substantially smaller.

Derived tyrannosaurids consistently possess a ventrally projecting jugal flange (Figure 8h). The development of the flange is restricted to the ventral surface of the jugal and extends from the mid-orbit region to the region ventral to the postorbital contact. Immature tyrannosaurid jugals (e.g. UALVP 61561) possess a similarly well-developed jugal flange, and this region appears to become increasingly rugose throughout ontogeny (e.g. TMP 2001.036.0001). Mature specimens of *Daspletosaurus* spp. appear to have some of the best-developed jugal flanges of any tyrannosaurid. This feature is notably conspicuous in TMP 2001.036.0001, where the anteroventral margin of the jugal flange is strongly concave and hook-like. In *Alioramus altai* (Brusatte et al., 2012) and *Daspletosaurus* spp., there is an accessory lateral rugosity dorsal to the jugal flange on the lateral surface.

The morphology of the surangular shelf, similar to that of other theropods and herrerasaurids, appears to have been conserved throughout tyrannosauroid evolution. The anteroposteriorly elongate shelf appears along the dorsal margin of the lateral surface of the surangular and projects laterally (Figure 8i). The shelf consistently arises anterior to the glenoid fossa and terminates ventral to the cornual process of the jugal but varies slightly in shape. In early branching tyrannosauroids (e.g. *Y. huali*), the surangular shelf is sinuous, whereas derived tyrannosaurids display an anteroposteriorly straight surangular shelf, exemplified by *Daspletosaurus* spp. and *Gorgosaurus libratus*.

3.2.13 | Dromaeosauridae

Dromaeosaurids show variation in the morphology of the ventral margin of the jugal. In *Dromaeosaurus albertensis* (AMNH FARB 5356), the jugal appears to lack a distinct ventral flange, instead showing a subtly convex ventral surface from the maxillary contact to the distal end of the ventral quadratojugal process. This morphology is akin to what is observed in allosauroids such as *Allosaurus* spp. and *Acr. atokensis*, but distinct from other dromaeosaurids. *Deinonychus antirrhopus* shows a prominent ventral flange ventral to the postorbital process (YPM 438, YPM 5232). Much like in *M. crenatissimus*, this is manifested as a mediolateral swelling that is widest anteriorly and tapers gradually posteriorly. In *Saurornitholestes langstoni* (TMP 1975.010.0005, Figure 8m) and velociraptorine taxa such as *Tsaagan mangas* (MPC-D 100/1015) and *Velociraptor* sp. (MPC-D 100/982), there is a distinct and anteroposteriorly elongate ventral flange anterior to the quadratojugal processes. In these taxa, the flange flares laterally and has a clear dorsolateral lip (Figure 8m). Ventromedially to this lip, there are a number of large foramina opening ventrally or anteroventrally (although these could not be observed in *T. mangas* due to overlying matrix). Foramina along the ventral to ventrolateral margin are known from other dromaeosaurids; however, the ventromedial placement appears unique to *S. langstoni* and velociraptorines (Currie & Evans, 2020, Figure 8n). The ventral quadratojugal processes in all dromaeosaurids observed appear to be thickened relative to the ventral margin of the suborbital ramus and even relative to the ventral flange where present.

The surangular of dromaeosaurids shows the typical theropod surangular shelf, whose lateral extent matches that of the ventral quadratojugal process of the jugal. In articulated specimens of most taxa, the shelf terminates anteriorly posterior to the ventral flange of the jugal, but in *D. albertensis*, the lateral surangular shelf extends further anterior. The posterior restriction of the lateral shelf in most dromaeosaurids (except *D. albertensis*) is similar to what is observed in tyrannosauroids.

3.2.14 | Oviraptorosauria

The zygomata of oviraptorids are slender and similar to the typical avian condition, being circular in cross-section and lacking obvious flanges or tuberosities, but retaining the ascending postorbital process seen in other non-avians (*Citipati osmolskae*, Clark et al., 2002; Wang & Hu, 2017). In the caenagnathid *Anzu wyliei* (UALVP 56672, casts of CM 78000 and 78001), the ventral margin of the jugal bears a deep longitudinal fossa bordered laterally and medially by distinct laminae. Approximately level with the jugal fossa of *A. wyliei* is a large projection of the dorsal surface of the surangular; a similar projection is seen in oviraptorids (Clark et al., 2002). However, this projection is medially oriented, and so is likely uninformative in reconstructing a laterally positioned tissue.

The surangular of *C. osmolskae* shows a reduced version of the typical theropod surangular shelf (Clark et al., 2002, figure 9 therein), located in the same general position as it is in other theropods. No such shelf is present on the posterior mandible of *A. wyliei* (UALVP 56672).

3.2.15 | Avialae

Large ventral flanges do not appear to occur on the jugals of Mesozoic avialans, but some subtler features could conceivably represent entheseal sites. Among specimens of the anchiornithid *Anchiornis huxleyi*, the ventral edge of the anterior process of the jugal has an undulating morphology in BMNHC PH804, whereas the jugals of BMNHC PH823 and PKUP V1068 flare slightly ventrally at the anterior end, and in BMNHC PH823, the body of the jugal also bears a sharp but small triangular flange (Pei et al., 2017). In *Archaeopteryx* and the independent juvenile enantiornithine IVPP V12707 (Figure 8k), the dorsal most part of the postorbital process of the jugal forms a posteroventrally directed peak, termed the 'corneal process' (Wang et al., 2021; Wang & Hu, 2017). In the ornithuromorph *Jianchangornis microdonta*, the jugal may form a sharp posteroventral corner (Zhou et al., 2009, figure 3 therein).

In addition to these various prominences, the lateral surface of the jugal bears some sort of depression in many non-ornithothoracine avialans, taking the form of an elongate groove in *Anchiornis* and *Archaeopteryx* (Pei et al., 2017; Wang & Hu, 2017). A prominent ridge along the ventral edge of the lateral surface of the jugal of *Caihong* may help to define a similar feature (Hu et al., 2018). An anteroposteriorly shorter depression is present near the midpoint of the anterior process of the jugal in *Jeholornis* (Hu et al., 2023).

In Mesozoic avialans, the surangular makes a substantial posterodorsal contribution to the mandible, as in non-avialan theropods. In some non-ornithothoracine avialans, the dorsal margin of the surangular can be seen to protrude as an overhanging ridge either laterally or medially (Hu et al., 2018, 2023; Pei et al., 2017; Rauhut et al., 2010; Wellnhofer, 2009), suggesting that the dorsal margin is mediolaterally thickened either to facilitate soft tissue attachments or simply to provide strength. *Jeholornis* is unusual in having a distinct anteroposteriorly oriented ridge on the lateral surface of the jugal, a short distance below the dorsal margin, although the dorsal margin also appears thickened over a short interval situated

somewhat more anteriorly (Hu et al., 2023, figure 8g,h therein). At least slight thickening of the dorsal margin of the surangular also appears to occur in some ornithothoracine birds (Bell & Chiappe, 2020; Wang et al., 2021; Zhou et al., 2008; Zhou et al., 2013).

3.3 | Modern histology

3.3.1 | Jugolacrimal ligament

The jugolacrimal ligament is captured longitudinally on the transverse plane, and its collagen fibres show a distinct anisotropic pattern under cross-polarised light. Collagen fibres of the jugolacrimal ligament are attached to the maxilla and the jugal bar in two ways adjacent to their sutural contact. First, the jugolacrimal ligament is anchored onto the osseous maxilla and jugal by discrete bundles of entheseal fibres, which run in multiple orientations, their relationship to the jugolacrimal ligament ranging from subparallel to nearly perpendicular. Second, along the maxillojugal suture, collagen fibres of the jugolacrimal ligament are anchored by, or transition into, entheseal fibres embedded within patches of fibrocartilage on both the maxilla and the jugal. The jugolacrimal ligament thus appears to have a fibrocartilaginous enthesis at the maxillojugal suture and a fibrous one away from the suture.

3.3.2 | Medial jugomandibular ligament

The medial jugomandibular ligament adheres to the lateral and ventral aspects of the posterior jugal bar (Figure 9a–e). Close to the quadrate, the medial jugomandibular ligament does not adhere to the jugal bar directly, but instead is connected to the bar by a patch of loose connective tissue (Figure 9f). Caudal to the synovial capsule of the quadratomandibular joint, the medial jugomandibular ligament is attached to the medial condyle of the articular (Figure 9g).

The medial jugomandibular ligament is attached to the cortex of the jugal bar by entheseal fibres with four discernible variations. First, on the rostral part of the lateral aspect of the jugal bar, discrete, subparallel and organised collagen fibres pass from the medial jugomandibular ligament into the lamellar layer of the jugal cortex, and generally terminate superficial to the deeper cortical layer rich in secondary osteons (Figure 9d,e). The cortical thickness of the jugal bar is only slightly reduced on its lateral side where the medial jugomandibular ligament is attached. Second, on the ventral aspect of the jugal bar, the medial jugomandibular ligament is directly attached to the osseous cortex and the lamellar layer is highly reduced at the attachment site or even fully absent (Figure 9a–c). Two groups of discrete entheseal fibres diverge at an acute angle to anchor the ligamentous body into the cortex of the jugal bar. The first group passes dorsomedially and the second group passes mediolaterally, and they form an interweaving network at the attachment site. Almost all observed entheseal fibres terminate superficial to the deeper layer rich in secondary osteons, as in the more rostral sections. However, entheseal fibres can be seen to pass between two neighbouring secondary osteons on at least one sampled section (Figure 9c), which may reflect incomplete remodelling of collagenous tissues. Alternatively, the entheseal fibres might have remained unmodified to provide sufficient support for the increased volume of the jugomandibular ligament near this location. Third, close to the quadrate, the medial jugomandibular ligament is connected to the jugal bar by a patch of irregular connective tissue (Figure 9f). Two groups of entheseal fibres organised at an obtuse angle, one trending ventromedially and the other ventrolaterally, are observed to anchor the ligamentous body. Entheseal fibres terminate at the cortical layer rich in secondary osteons, as at the more rostral attachment sites. Fourth, at the quadratomandibular joint, seemingly unmodified bundles of collagen fibres continuous with those of the medial jugomandibular ligament insert deep into the bone of the medial condyle of the articular (Figure 9g). The entheseal fibres at this location likely represent a part of the medial jugomandibular ligament that is buried within the osseous tissue of the articular. Unlike at more rostral attachment sites, a group of entheseal fibres that appear to exist solely for anchoring the medial jugomandibular ligament is not observed, which may be influenced by the plane of section in our sample. At all sites of attachment in our sample, the medial jugomandibular ligament is attached to bone by entheseal fibres with no fibrocartilage present, and this ligamentous attachment can therefore be classified as a fibrous enthesis.

3.3.3 | Histological correlates of entheses

Three histological features visible in the extant histological sections made in this study may indicate entheseal attachment: First, a region of cortex consisting mostly of secondary osteons with a thin external layer of lamellar or primary bone; second, an assemblage of subparallel entheseal fibres within the cortex; and finally, an assemblage of entheseal fibres within the cortex that exhibit two distinct orientations.

While the jugal bar was the primary focus of our extant histology work, entheseal fibres were also observed in tendinous and fleshy attachments of muscles to structures other than the jugal bar in our slides (Figure 10a–c). The attachment of the *m. pterygoideus ventralis* to the articular, in particular, strongly resembles the attachment of the medial jugomandibular ligament in two ways (Figure 10c): first, the tendon of *m. pterygoideus ventralis* makes direct contact with the secondary osteons, and second, the collagen fibres of the tendon pass into the osseous tissue of the articular.

3.4 | Paleohistology

3.4.1 | Ceratopsidae

An outermost layer of abundant subsurface fibres was visible on every section of ceratopsian cranial bone (Figure 11), external to

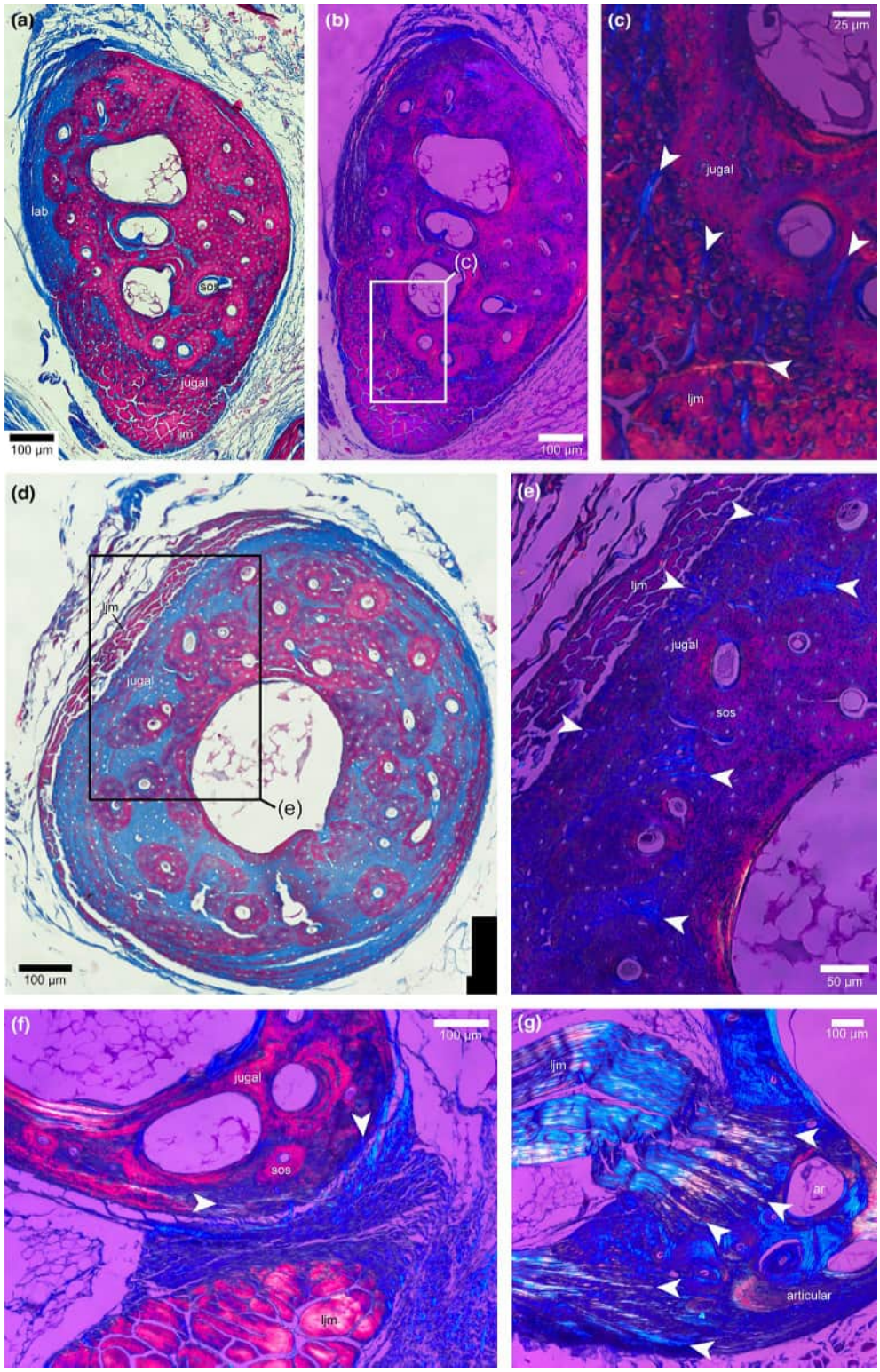

FIGURE 9 Histological thin section of left partial head in chicken *Gallus gallus* (UAMZ unnumbered). (a) Transverse/subtransverse thin section of jugal bar caudal to jugoquadratojugal suture, showing ventral attachment site of medial jugomandibular ligament; (b, c) close-up on jugal bar showing entheseal fibres anchoring medial jugomandibular ligament; (d) transverse/subtransverse thin section of jugal bar caudal to jugoquadratojugal suture, showing lateral attachment site of medial jugomandibular ligament; (e) close-up on lateral aspect of jugal bar showing entheseal fibres anchoring medial jugomandibular ligament; (f) transverse/subtransverse thin section of jugal bar adjacent to quadrate, showing attachment site of medial jugomandibular ligament bridged by dense irregular connective tissues; (g) transverse/subtransverse thin section adjacent to quadromandibular joint, showing attachment site of medial jugomendibular ligament at medial condyle of articular. Panels B and D are captured under normal light, and remaining panels are captured under cross-polarised light. White triangles point at entheseal fibres. Ar, articular; ju, jugal bar; lab, lamellar bone; ljl, jugolacrimal ligament; ljm, medial jugomandibular ligament; mx, maxilla, sos, secondary osteon.

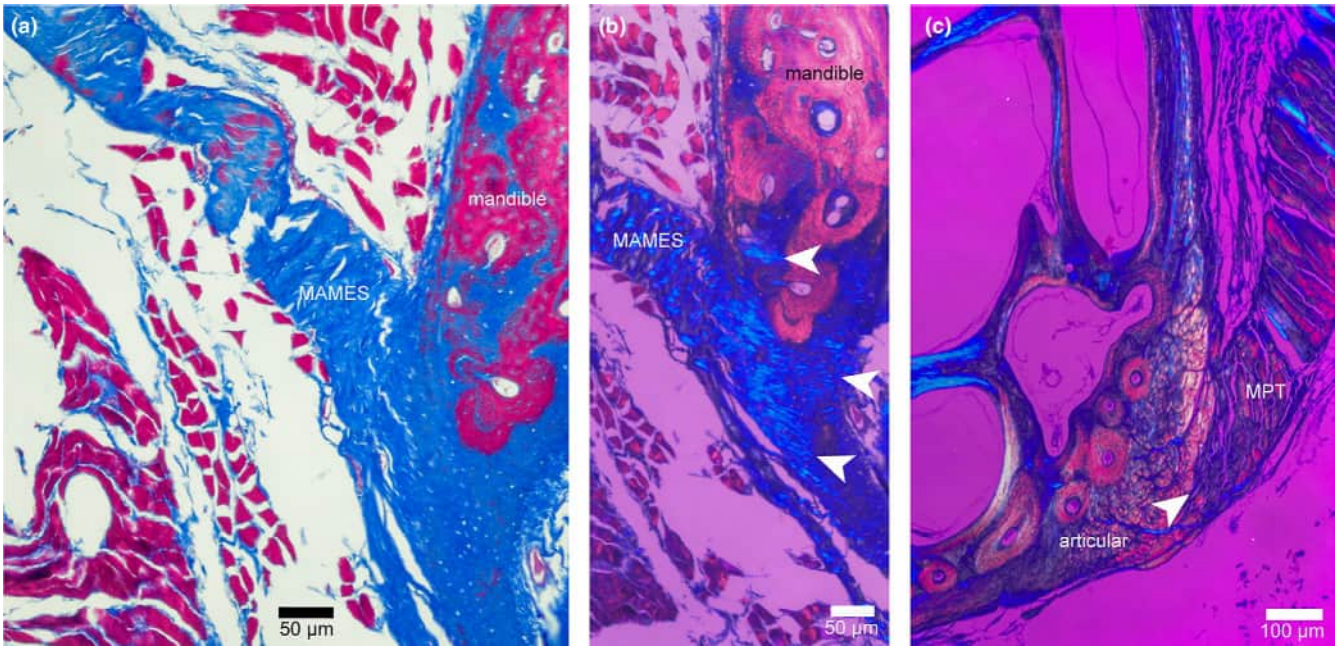

FIGURE 10 Histological thin section of right partial head in chicken *Gallus gallus* (UAMZ unnumbered). (a, b) Transverse/subtransverse thin section at the middle part of mandible, showing tendinous attachment (a) and its entheseal fibres (b); (c) transverse/subtransverse thin section at the caudal part of mandible, showing tendinous attachment. (a) is captured under normal light, and (b, c) are captured under cross-polarised light. MAMES, *m. adductor mandibulae externus superficialis*; ar, articular; md, mandible; MPT, *m. pterygoideus ventralis*; sos, secondary osteon.

the main cortex of secondary osteons. The fibres observed here occur in one of two distinct configurations: robust bundles distinctly angled relative to each other in a plywood-like arrangement (Figure 11c), similar to that seen in the osteoderms of trionychid turtle shells (Scheyer et al., 2007), and (2) a uniformly spaced arrangement of individual fibres, as observed in the extant samples. The first, plywood-like morphology, is notably present only on rugose subdermal surfaces (e.g. lateral surfaces of the jugal and surangular), whereas the continuous uniform fibres are restricted to the medial surface of the jugal (TMP 1992.036.0929, Figure 11b) and the dorsal and dorsomedial surfaces of the surangular ridge (TMP 1980.018.0159, TMP 1980.018.0253). These fibres point ventromedially on the medial surface of the jugal TMP 1992.036.0929 and are less visible than the more distinct plywood-like fibres on the lateral surface (Figure 11a). On the anterior margin of this jugal, along the slight anteroventral ridge, both the plywood and uniform arrangements of fibres are present, the latter orienting anteroventrally. On the surangular ridge, parallel fibres captured in two subtransverse sections of the same surangular (TMP 1980.018.0253) orient mostly dorsally or dorsolaterally (Figure 11d). Two individuals (TMP 1980.018.0159, TMP 1980.018.0253) show dorsally or posterodorsally oriented fibres in the parasagittal section; parallel fibres are found in both, but only one (TMP 1980.018.0159) shows the plywood-like arrangement on part of its surface.

Fibre orientations indicate that the tensile load imposed by the attached soft tissue structure was primarily directed ventrally, medially and anteriorly in the case of the jugal, and dorsally, laterally and anteriorly in the case of the surangular. The surangular fibres in TMP 1980.018.0159 and TMP 1980.018.0253 notably do not predominantly angle dorsomedially into the temporal region (Figure 11d), arguing against an origin from the temporal adductors. Overall, the fibres in the sectioned ceratopsian bones indicate complementary soft tissue attachments on the anterior and medial surfaces of the jugal and on the surangular ridge (Figure 3a).

3.4.2 | Hadrosauridae

Each sectioned hadrosaurid element shows an outermost layer of bone rich in subsurface fibres external to the osteon-rich cortex (Figure 12). Several secondary osteons interrupt the fibrous outer layer, and some fibres can be observed to curve around the osteons in the jugal UALVP 55263. Along the jugal flange of TMP 1986.078.0005, the medial side has a high concentration of hoop-shaped osteons, while the lateral side has more dispersed-type osteons (Skedros et al., 2009). The fibres preserved in all hadrosaurid sections closely resemble the entheseal fibres seen in extant sections and the parallel fibres in ceratopsid sections (Figure 11b). Occasionally, fibres are overlaid crosswise to each other; this differs from the more concentrated and not-overlaid plywood-like arrangement seen in ceratopsids, instead resembling the crossed orientations seen in some extant sections (Figure 9f). Fibres visible in subtransverse sections of hadrosaurid jugal flanges (TMP 1986.078.0005, UALVP 55263, Figure 12a,b) orient ventrally; those along the ventrolateral and ventromedial surfaces, respectively,

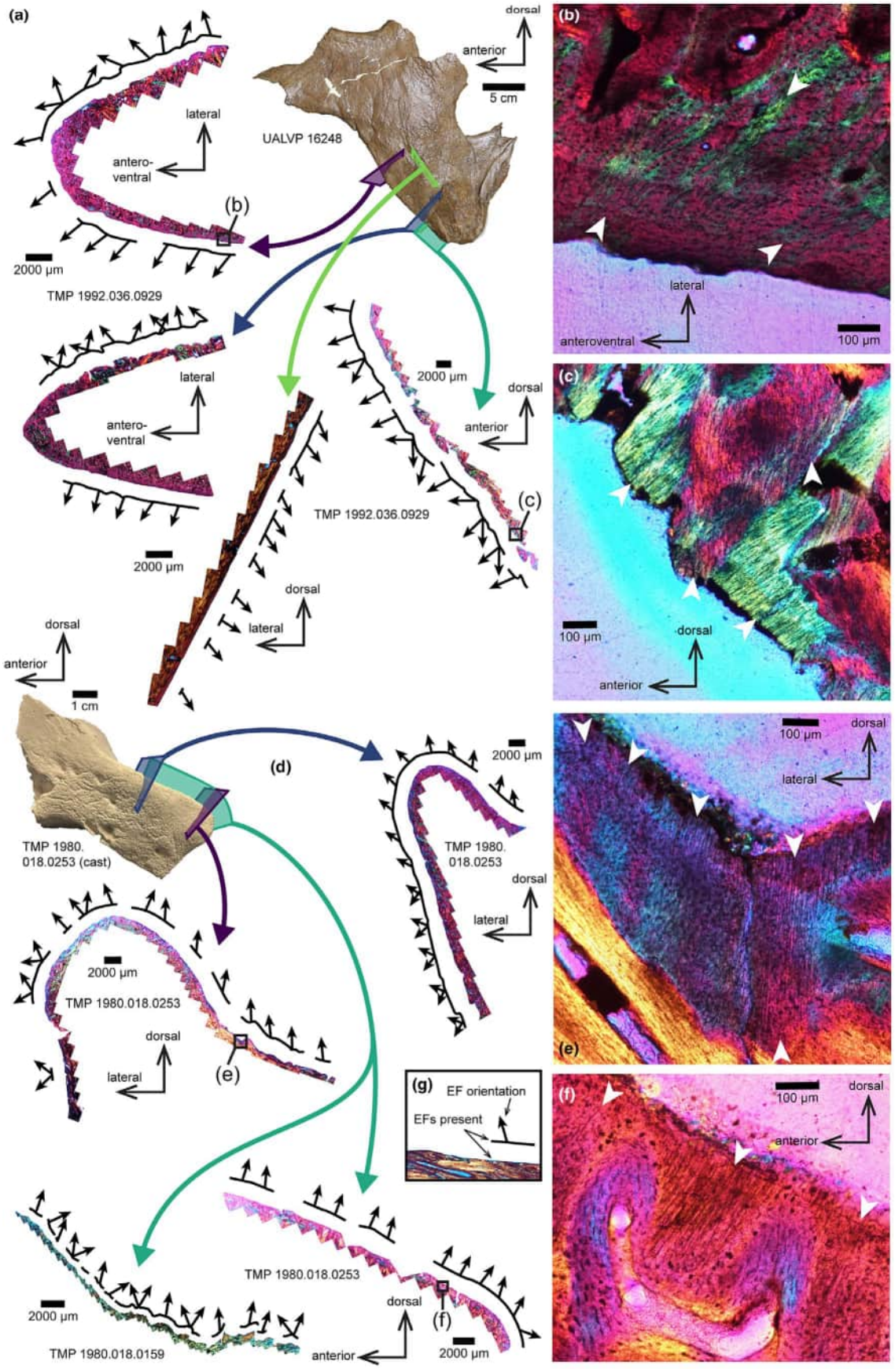

FIGURE 11 Histology of ceratopsid cranial bones. (a–c) Histological sections of a ceratopsid jugal; (d–f) histological sections of ceratopsid surangulars; (g) legend. White arrows indicate entheseal fibres. EF, entheseal fibres.

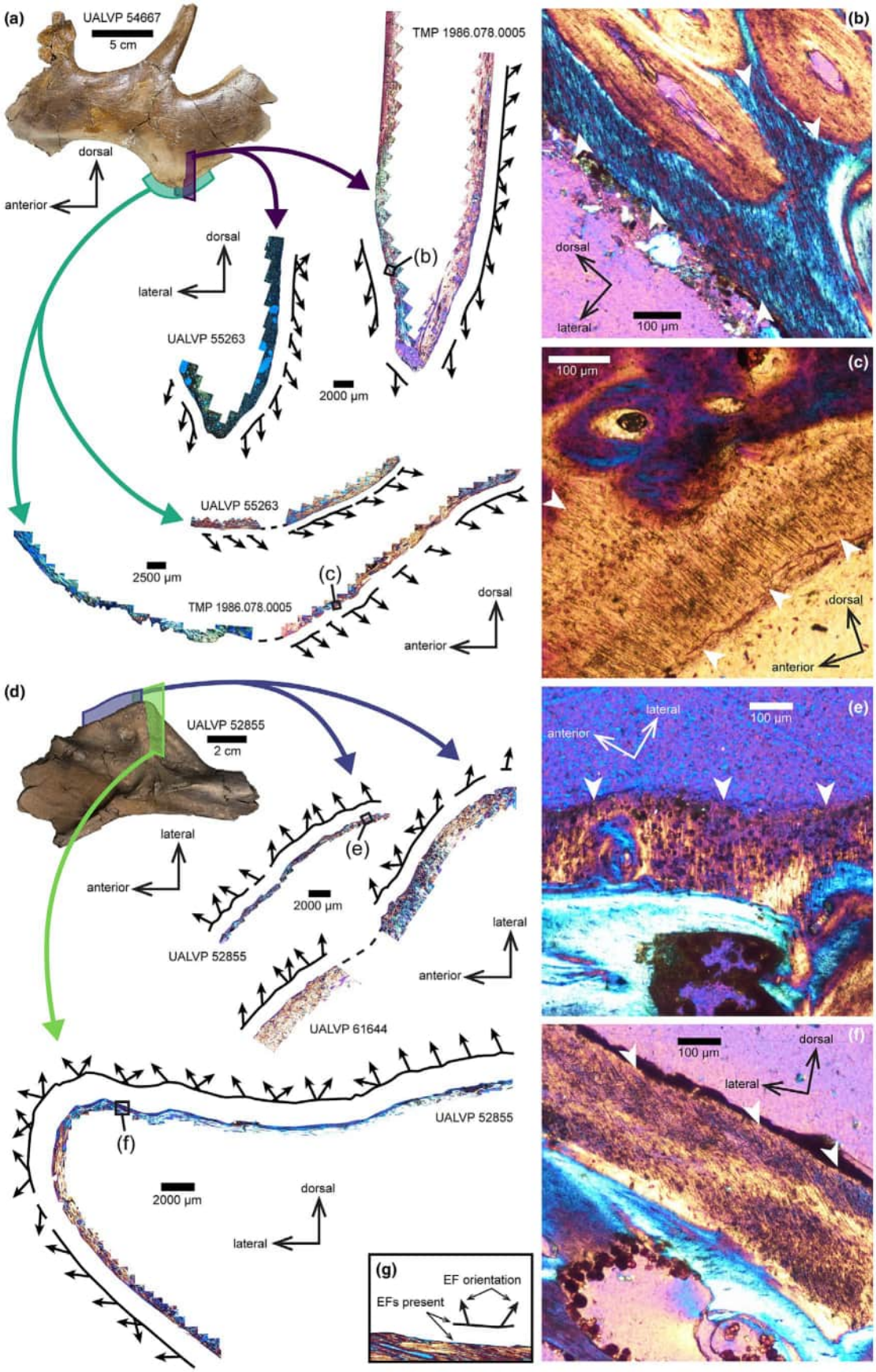

FIGURE 12 Histology of hadrosaurid cranial bones. (a–c) Histological sections of hadrosaurid jugals; (d–f) histological sections of hadrosaurid surangulars; (g) legend. White arrows indicate entheseal fibres. EF, entheseal fibres.

point ventrolaterally and ventromedially. In both individuals, fibres are present all over the medial surface of the jugal flange. However, the fibres on the lateral surface are restricted to the sulcate posteroventral margin of the flange and do not occur dorsal to this margin. In parasagittal sections, the fibres orient posteroventrally and are only visible posterior to the ventral apex of the flange in TMP 1986.078.0005 (Figure 12a,c). The fibres in this specimen are almost universally parallel to macroscopic striations visible on the lateral surface of the jugal flange in the same specimen (Figure 13b). Along the surangular flange (UALVP 52855, UALVP 62644), anterodorsally oriented fibres are visible in the parasagittal sections from two individuals (Figure 12d). Transverse sections of the flange in UALVP 52855 show fibres extending in various directions from the ventrolateral and dorsal surfaces of the flange, but the majority point dorsolaterally.

The jugal flange presents good evidence for an enthesis, with a primary loading axis directed posteriorly, ventrally and medially. The surangular presents some evidence for the same, with a primary loading axis directed dorsally, anteriorly and laterally. These orientations are complementary to each other; the jugal fibres orient towards the surangular, and those on the surangular orient towards the jugal, supporting our hypothesis for soft tissue joining these entheses (Figure 3b). The majority of entheseal fibres are located on the medial surface of the jugal flange. As in ceratopsids, there is no evidence for an enthesis on the surangular flange with a loading angle oriented dorsomedially towards the temporal region.

3.4.3 | Tyrannosauridae

Both sectioned tyrannosaurid jugals (TMP 1991.163.0001, TMP 2000.012.0011) and the tyrannosaurid surangular (TMP 2000.012.0011) show an outer layer of fibrous bone that resembles entheseal fibres in extant sections (Figure 14a–d,f,g). In transverse sections of the jugals (Figure 14a–c), multiple stacked layers of this fibrous bone can be observed with the fibres running parallel to the outer surface, although multiple fibres clearly span in between these layers. Some fibres appear to bend around secondary osteons (Figure 14c). Sets of these fibres can be observed to run crosswise to each other in transverse view, resembling similar overlaid orientations in the hadrosaur sections and not the concentrated plywood-like orientation seen in ceratopsid subdermal bone. The most conspicuous fibres in jugal transverse sections orient ventromedially. In the parasagittal section of TMP 2000.012.0011 (Figure 14a,e), the fibres are uniformly posteroventral in orientation. These fibres are generally parallel to the macroscopic striations on the lateral jugal surface of the same specimen (Figure 13a), similar to the hadrosaur jugal TMP 1986.078.0005 (Figure 14b). Fibres continue this orientation into the multiple protrusions that create the rugosities visible macroscopically on the jugal flange of this specimen. Unlike the hadrosaur and ceratopsian sections, in which the fibres form a near-continuous outer layer, the tyrannosaur sections have a layer of fibres that are not continuous in that they are interrupted by non-fibrous bone. Tyrannosaur jugal TMP 1991.163.0001 is from

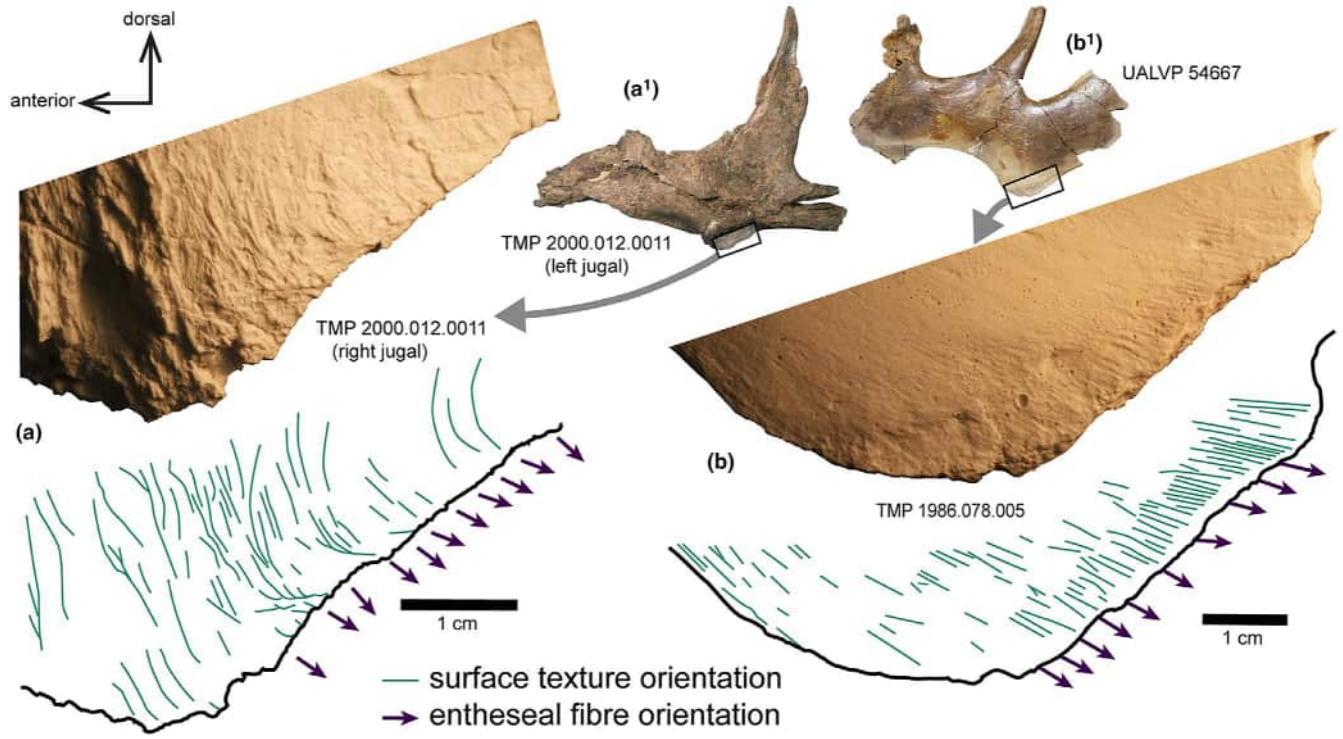

FIGURE 13 Surface texturing compared to entheseal fibres of (a) tyrannosaurid and (b) hadrosaurid jugals. Insets (a^1, b^1) show whole jugals. (a, b) show casts of jugals that were sectioned to produce the line drawings below.

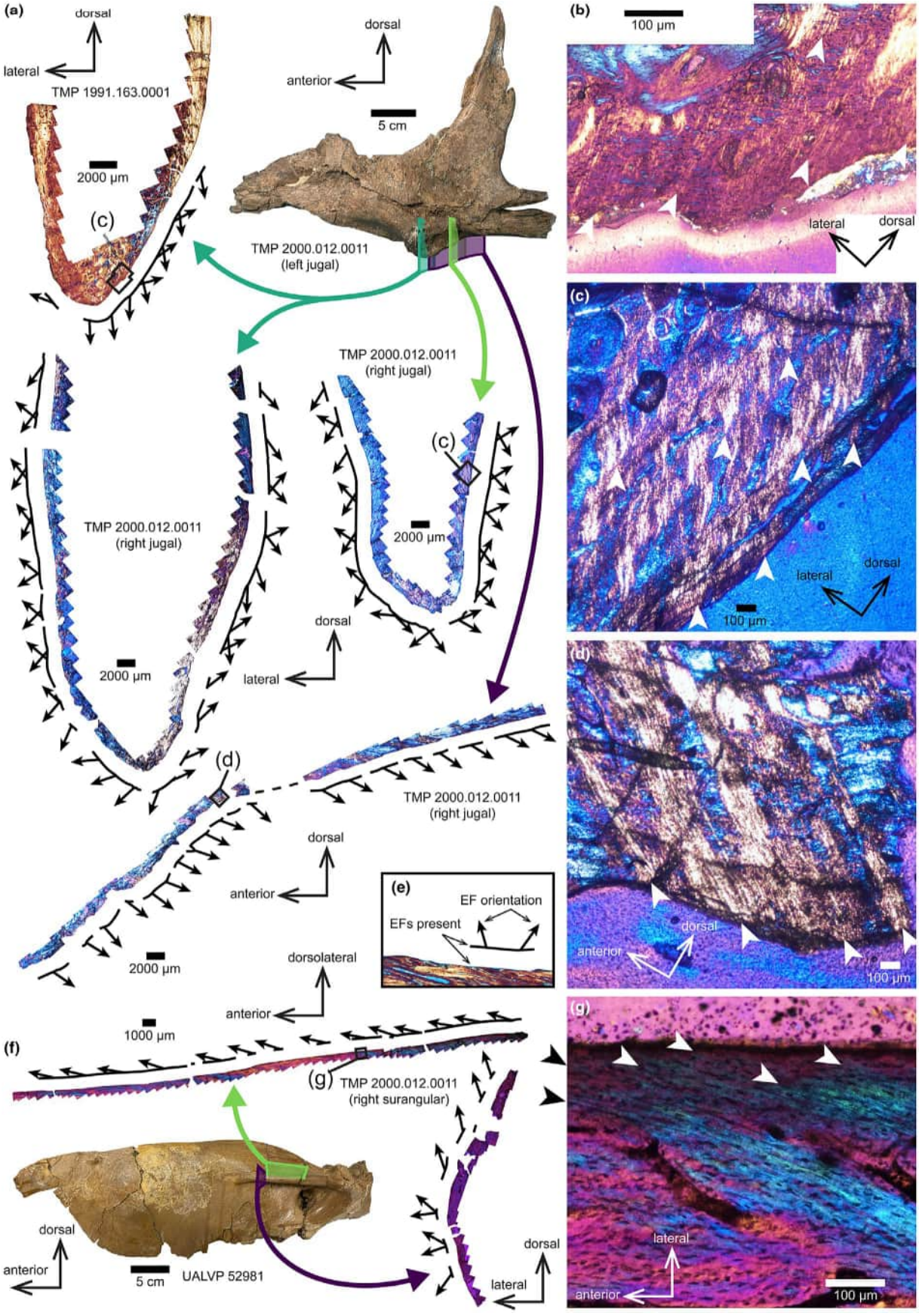

FIGURE 14 Histology of tyrannosaurid cranial bones. (a–d) Histological sections of tyrannosaurid jugals; (e) legend; (f, g) histological sections of a tyrannosaurid surangular. White arrows indicate entheseal fibres. EF, entheseal fibres.

a much smaller and likely more immature individual than jugal TMP 2000.012.0011. The scale of the fibres visible in these specimens is similarly different, the fibres in the smaller jugal (TMP 1991.163.0001) being much smaller in diameter than those in both the larger tyrannosaurid jugal (TMP 2000.012.0011) and the previously examined ceratopsid and hadrosaurid bones. The larger tyrannosaurid jugal (TMP 2000.012.0011) has coarser fibres than those seen in the other ceratopsid and hadrosaurid bones. A transverse section of the surangular shelf shows abundant fibres pointing dorsolaterally along its dorsal portion and ventrolaterally along its ventral portion, with some mixture of orientations near the middle (Figure 14f). Coronal sectioning of the dorsal portion of the surangular shelf shows a dense arrangement of fibres that is nearly continuous across its entire surface (Figure 14f,g). All of these fibres are parallel and oriented strongly anteriorly and slightly dorsally. The fibres observed here are of a similar size to those in the jugal of the same specimen (Figure 14d,g).

The tyrannosaurid jugals sectioned here provide evidence for a soft tissue enthesis on the jugal flange of these individuals, with the soft tissue exerting a tensile load directed primarily ventrally, medially and posteriorly. Similarly, the surangular shows evidence for an enthesis on the lateral shelf, with the soft tissue exerting a tensile load directed primarily anteriorly, dorsally and laterally. In parasagittal sections in particular, the fibres in the jugal and surangular entheses of the same individual (TMP 2000.012.0011) orient directly towards each other, supporting a single soft tissue structure connecting these entheses (Figure 3c). The ventrally oriented fibres visible in the transverse section of the surangular shelf may result from the attachment of the *M. pterygoideus ventralis*, though additional histology of this region is required to test this.

4 | DISCUSSION

4.1 | Tissue reconstruction

The zygomatic enthesis for the exoparia is anteriorly positioned relative to the mandibular enthesis in early branching dinosaurs, theropods, early branching ornithischians, ornithopods and thyreophorans. This implies that the exoparia exerted an anterodorsally oriented tensile force on the mandible and a posteroventrally oriented one on the zygoma (Figure 15a,b,d,e). The apparent orientation in pachycephalosaurians and ceratopsids would have been more dorsoventral, with less horizontal skew (Figure 15f). In several sauropod specimens that preserve well-developed zygomatic flanges (CMC VP 7180, MZSP-Pv 807, ZDM T 5403), the flange extends anteroventrally and the posterior mandible lacks an obvious flange, differing from other dinosaur clades studied here and possibly indicating an anteroventral–posterodorsal orientation for the exoparia (Figure 15c).

In most early branching dinosaurs (herrerasaurids, silesaurids, early branching sauropodomorphs, early branching theropods) the zygomatic enthesis is associated with an anteroposteriorly long ridge and flange along the lateral surface of the jugal (Figure 16). In several more derived lineages, the enthesis is modified into large flanges (heterodontosaurs, ornithopods, sauropods) or rugose patches (theropods, marginocephalians). Similarly, the mandibular enthesis ranges from anteroposteriorly long shelves (herrerasaurids, theropods) to more compact flanges (ornithischians). This suggests a sufficient degree of morphological diversity in the exoparia to create such diversity in its attachment sites. Anteroposteriorly long entheses may indicate attachments for more dispersed and sheetlike tissue, while anteroposteriorly compact flanges may indicate attachments for narrower bands of tissue.

The tyrannosaurid jugal flange and lateral rugosity have previously been interpreted as bases for cornified ornaments (Brusatte et al., 2012; Carr et al., 2017). In the published literature, cornified integument is often bound to underlying bone by entheseal fibres oriented perpendicular to the bone surface (de Buffrénil et al., 2010; Kirby et al., 2020; Sena et al., 2023), such that fibres under a convex bone surface are not parallel to each other but show a radiating orientation. The fibres observed in our sections of the jugal flange are oriented subparallel to each other and not perpendicular to the bone surface, resembling muscular and ligamentous attachments in extant sections (Figure 4a,b,e). This resemblance, taken with the topological consistency of the jugal flange in tyrannosaurids with similar flanges and rugosities across Dinosauria (Figure 16), and the complementary fibres pointing to this region in the surangular (Figure 14f,g) indicate that this feature represented an entheseal site instead of the base of a ventrolaterally projecting cornified ornament. The laterally projecting jugal rugosities of *Alioramus altai* (Brusatte et al., 2012) and possibly *Qianzhousaurus sinensis* (Foster et al., 2021) may have supported cornified horns, unlike in other tyrannosaurids, or instead represent exostoses of the exoparial enthesis.

4.2 | Homology of the exoparia and resulting implications

We provide the term 'exoparia' to describe the strong evidence for connective tissue structures connecting the zygomata to the mandibles of, at minimum, the majority of known dinosaur taxa. Since certain criteria for examining the homology of these features to each other cannot be applied here, such as the topology of blood vessels and nerves (Holliday & Witmer, 2007) and developmental sequences (Tokita, 2004), it is difficult to properly test the homology of the exoparia between different dinosaur clades. A single tissue from a single origin is the most parsimonious solution to this case, but (as discussed at the end of this section) myology often does not act parsimoniously. At present, we hypothesise the exoparia to be a single homologous tissue in dinosaurs, but highlight the possibility that it may have multiple origins and/or have derived into distinct subdivisions throughout dinosaurian evolution.

In extant birds, two ligaments (the cruciate jugomandibular ligaments) connect the zygoma to the mandible. These twin ligaments originate on the zygoma laterally and medially to insert on the

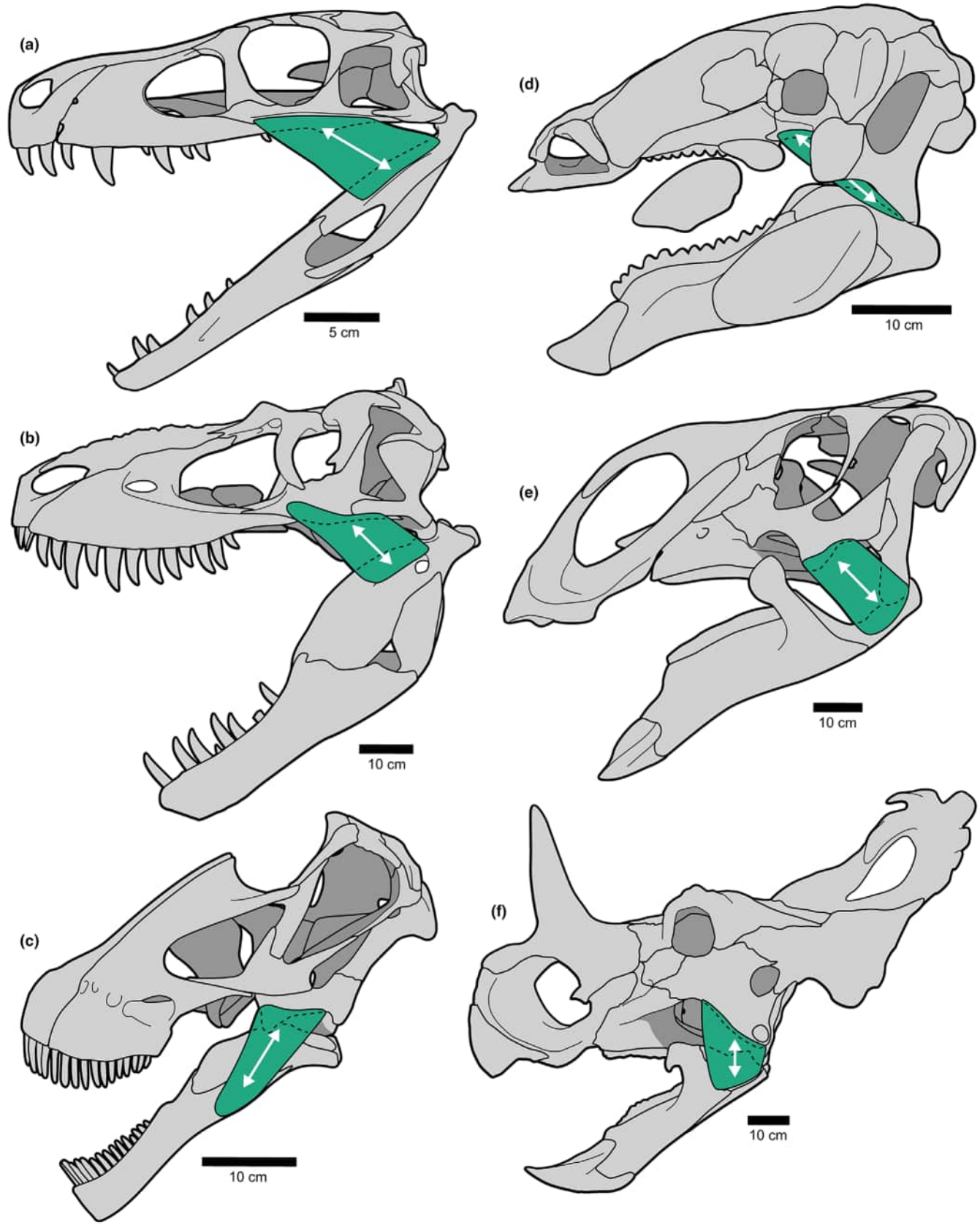

FIGURE 15 Reconstructed size and primary orientation of the exoparia in representative dinosaur skulls, all in left lateral view. (a) Herrerasauridae, *Gnathovorax cabreirai* (illustrated from Pacheco et al., 2019a, 2019b); (b) Theropoda, Tyrannosauridae sp. (illustrated from UALVP 52981); (c) Sauropoda, *Tapuiasaurus macedoi* (redrawn from Wilson et al., 2016); (d) Thyreophora, *Edmontonia rugosidens* (illustrated from TMP 1998.098.0001; UALVP 16249, 55668 and Vickaryous, 2006); (e) Ornithopoda, *Brachylophosaurus canadensis* (illustrated from CMN 8893); (f) Marginocephalia, *Centrosaurus apertus* (illustrated from UALVP 16248).

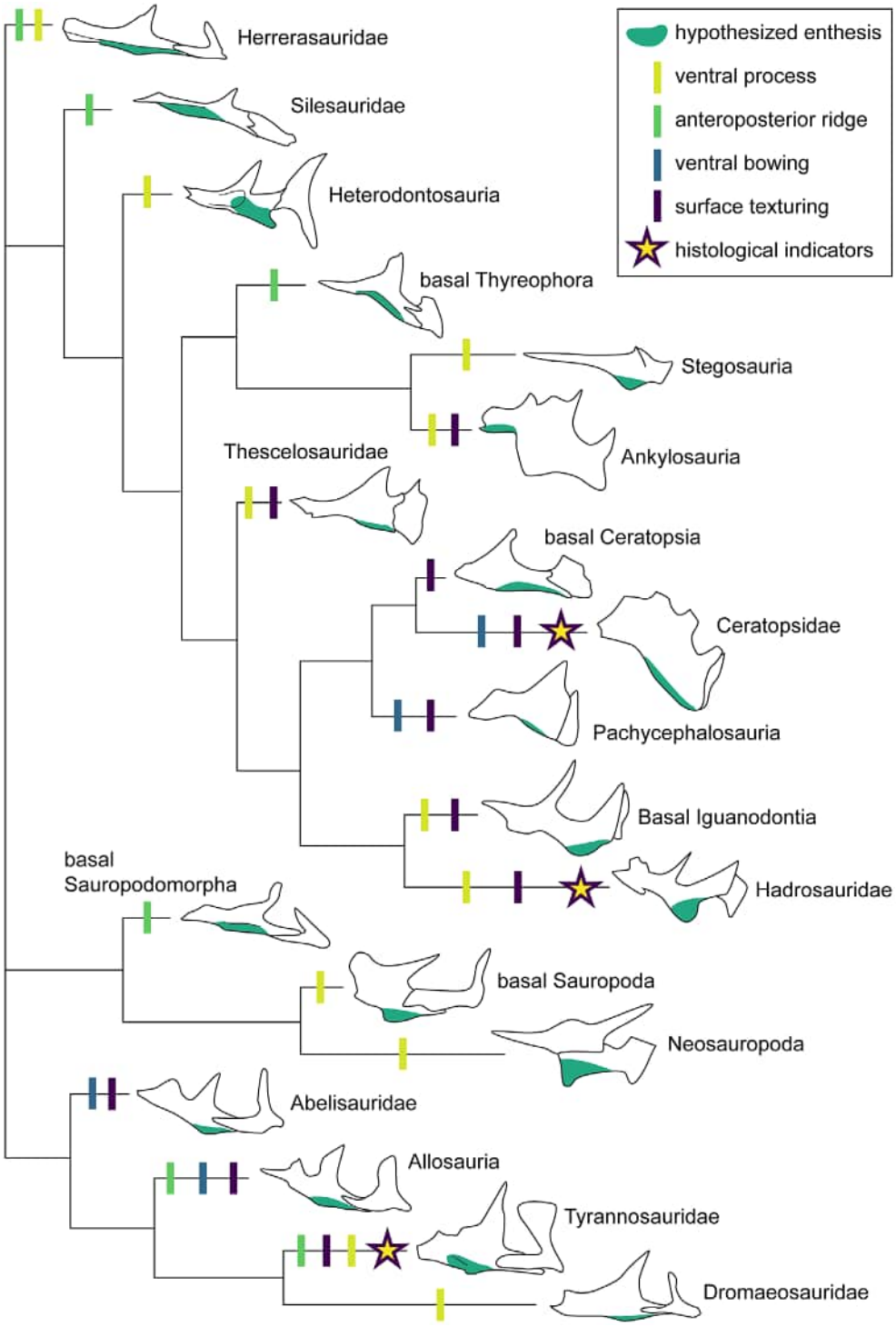

FIGURE 16 Distribution of entheseal indicators on dinosaur zygomata (all left sides in lateral view). Phylogenetic relationships are compiled from sources mentioned in the Results section and from Weishampel et al. (2004). Illustrations not to scale.

mandible. In this way, they are similar to the collateral ligaments that flank the crocodilian craniomandibular joint; the possibility of homology between these avian and crocodilian ligament sets warrants investigation. There remains the further possibility that one or both of these ligaments are homologous to the exoparia.

The postorbital ligament connects the avian postorbital region to the mandible. Extant birds have lost the plesiomorphic osseous connection between the postorbital and jugal; it is conceivable that a tissue inserting on the jugal could have migrated to a postorbital attachment in birds before this connection was lost. Interestingly, several early branching fossil avian taxa show a distinct, ventrally oriented 'corneal process' on the ascending postorbital process of the jugal (Figure 8k). If the corneal process was associated with the jugal attachment of the exoparia, indicating displacement of the attachment onto the ascending process, the attachment might subsequently have shifted onto the postorbital. Under this so far untested hypothesis,

the exoparia would be homologous to the avian postorbital ligament. This or other ligamentous homologies would not necessitate a ligamentous identity for the exoparia, as transformational homology between a muscle and ligament could conceivably result from gradual reduction of the muscular component and corresponding increase in the tendinous component of a muscle. The aforementioned close resemblance between the gross structures of the jugal flange in several of the dinosaurs examined in this study and the muscular entheses in modern vertebrates would support such a hypothesis.

Given the absence of any firmly established homologue in extant archosaurs, specific application of the EPB to muscles or ligaments linking the zygoma and mandible would not recover the presence of the exoparia in dinosaurs, which would be classified as a Level II or III inference (Witmer, 1995). The results of this study therefore provide abundant evidence for a tissue that would not be predicted using the EPB approach. The external osteological indicators presented herein are not subtle, and numerous authors have noted their resemblance to entheseal features (Holliday, 2009; Lull & Wright, 1942; Norman, 1986; Sereno, 2012; Sereno et al., 2010; Tsogtbaatar et al., 2019; Weishampel et al., 2003), yet only studies that did not use the EPB have presented similar conclusions (Lull & Wright, 1942; Sereno, 2012; Sereno et al., 2010). Witmer (1995) argued that the '*…extant phylogenetic bracket allows formulation of hypotheses about the soft-tissue relations of extinct taxa that may be tested by reference to the known osteological correlates of the soft tissues in fossil taxa enclosed by the bracket*', and that soft tissues under Level II and III inferences '*… may be regarded as unfounded. However, speculation may be fruitful (and even correct) if there is compelling morphological evidence for a particular soft-anatomical feature*'.

The evidence presented here for the exoparia argues for the testing of EPB-generated hypotheses using correlates of unpredicted soft tissues in addition to predicted soft tissues, instead of dismissing the former as speculative. It also serves as a reminder that EPB-derived reconstructions remain hypotheses to be tested, regardless of the plethora of studies that have used such reconstructions as established base models to generate functional and behavioural results (e.g. Gignac & Erickson, 2017; Snively & Russell, 2007). This is especially relevant in the case of dinosaurs; the EPB for this clade encompasses a time gap of over 100 million years during which an exceptional amount of morphological diversification is known to have occurred. Limiting the possibilities of soft tissue evolution through deep time to only what is expressed in modern taxa ignores the inevitability of a more complex past than the present can demonstrate. The massive amount of myological variation (muscle presences, absences and structural differences) that exists between and within modern avian species (George & Berger, 1966; Maxwell & Larsson, 2007; Tokita, 2004) also argues against the uniform application of one suite of soft tissues to non-avian dinosaurs; within our own sample, the exoparial entheses are morphologically variable and occasionally absent, indicating rich diversity in this feature alone. Reconstructions of dinosaur soft tissues should therefore critically examine phylogenetically derived results using multiple methods of testing (e.g. osteology, histology) before additional functional and behavioral hypotheses are built upon them (see Witmer, 1995, figure 2.1 therein).

4.3 | Functional implications

Muscles joining the zygoma and mandible have evolved independently in mammals (Lautenschlager et al., 2017) and psittaciform birds (Tokita, 2004). In mammals, the *M. masseter* aids in mastication, and many taxa have modified and subdivided this muscle for more specialised mastication (Grossnickle et al., 2022); in birds, the functional anatomy of the *M. pseudomasseter* is understudied.

Several extant groups possess ligamentous soft tissue connecting the zygoma to the mandible, such as birds (Bout & Zweers, 2001), crocodilians (Saber & Hassanin, 2014), squamates (Herrel et al., 1998; Iordansky, 1997, 2016) and mammals (temporomandibular ligament in human anatomy; Helland, 1980). Although these ligamentous tissues are not universally present in amniotes, as a whole, they serve to stabilise the mandible and prevent excessive translational movements during jaw protraction or retraction (Bout & Zweers, 2001; Helland, 1980), or maintain contact between the jaw and skull at the temporomandibular joint throughout its range of motion (Osborn, 1989). The size and morphology of these ligaments therefore vary dramatically between taxa. Animals with little translational mobility at the jaw joint tend to have reduced ligaments, while animals with more movement of the jaw or kinetic skulls tend to have larger ligaments (e.g. *Meleagris gallopavo*, Venkatesan et al., 2015).

The diversity observed here in the proposed attachment sites of the exoparia in extinct dinosaurs may be indicative of biomechanical differences among the jaws of these animals. This is consistent with previously proposed diverse reconstructions of dinosaur jaw musculature that mirror inferred differences in feeding habits (Nabavizadeh, 2020a). In each reconstruction of the exoparia, the proposed mandibular entheses are restricted to the lateral margin of the surangular, and so the body of the exoparia as reconstructed here would likely not have physically interfered with the function of the other mandibular adducting tissues (aside from reducing their mandibular attachment areas compared to recent reconstructions, e.g. Holliday, 2009). By far the best-developed cranial attachment sites for the exoparia were observed in hadrosaurids and ceratopsids, which are hypothesised to have had relatively mobile jaws that both moved anteroposteriorly and rotated about their long axes, particularly in hadrosaurids (Nabavizadeh, 2014). The anteroposterior orientation of the exoparia in these taxa is consistent with previously hypothesised jaw muscle orientations, which suggest that hadrosaurids and ceratopsids, and some early diverging neoceratopsians, had strong posteriorly directed jaw muscles (Mallon & Anderson, 2015; Nabavizadeh, 2016; Figure 1d). These hypothesised muscle vectors are supported by dental microwear, which suggests hadrosaurids and neoceratopsians used palinal jaw movements during food processing (Mallon & Anderson, 2014; Varriale, 2016). The posterior component of the force exerted by the jaw muscles would therefore have required some form of stabilisation to prevent excessive palinal movement of

the jaw, as seen in extant groups. A muscular or ligamentous identity for the exoparia could have provided an anterior stabilising vector during the palinal jaw stroke, but only a muscular exoparia could have actively contributed to palinal movement by pulling the mandible anteriorly. Biomechanical modelling would help test these hypotheses.

AUTHOR CONTRIBUTIONS

HSS conceptualised and led the study. HSS and YW generated histological data. HSS, YW and SAW analysed histological data. HSS, TWD, MJP, CCC, ADD and CS analysed morphological data. HSS and YW generated figures. CS provided project administration. All authors drafted the manuscript.

ACKNOWLEDGEMENTS

We express our thorough gratitude to Ali Nabavizadeh and an anonymous reviewer for their helpful reviews that improved this manuscript; Mateusz Wosik for handling our manuscript; Michael Caldwell for supervising undergraduate work by HSS that led to this project and for providing access to microscope and imaging software; Robin Sissons for providing instruction in molding and casting; Christiana Garros for providing instruction in paleohistology; Howard Gibbins, Clive Coy, Lisa Budney, Philip Currie (University of Alberta), Brandon Strilisky, Tom Courtenay and Jillian Richard (TMP), Kevin Seymour, Ian Morrison and Brian Iwama (ROM), and Scott Rufolo and Shyong En Pan (CMN) for access to collections and/or histological specimen sourcing; Christophe Mallet and Felippo Bertozzo (IRSNB) for data and discussions regarding *Iguanodon* jugals; Casey Holliday, Ali Nabavizadeh and Larry Witmer for discussions on craniomandibular soft tissues; Al Lindoe for custom cutting microscope slides; Greg Funston for discussions on histology and oviraptorosaur cranial morphology; Rodrigo Müller for specimen photos of *Gnathovorax*; Juan Canale for specimen photos of *Meraxes*; Philip Currie for specimen photos of *Mapusaurus* and *Tyrannotitan* jugals; James Napoli and the North Carolina Museum of Natural Sciences for specimen photos and surface scans of *Thescelosaurus*; Xu Xing for specimen photos of *Lufengosaurus*; Peng Guangzhao for specimen photos of *Shunosaurus*; Jeff Wilson Mantilla for specimen photos of *Tapuiasaurus*; Emily Lessner for CT scans of *Allosaurus*; Matthew Lamanna for surface scans of *Daemonosaurus*; Patrick O'Connor for surface scans of *Majungasaurus*; Bernhard Zipfel for CT scans of *Massospondylus*, and Kimberly Chapelle for surface scans of *Massospondylus* and *Ngwevu*. Attribution for specimens accessed through the Morphosource repository (*Allosaurus*, *Daemonosaurus*, *Majungasaurus*, *Massospondylus*, *Ngwevu*) are visible in Table S1. HSS is funded by a Canadian Graduate Scholarship—Master's award and CS is funded by a Discovery Grant, both courtesy of the National Science and Engineering Research Council of Canada.

DATA AVAILABILITY STATEMENT

High-quality images of the histological slides generated for this study are openly available in figshare at http://doi.org/10.6084/m9.figshare.28385573, and the slides themselves are accessioned in the TMP and UALVP collections. Source information on the 3D specimens studied herein can be found in the supplementary material.

ORCID

Henry S. Sharpe https://orcid.org/0009-0008-4757-995X
S. Amber Whitebone https://orcid.org/0000-0003-4962-2444

REFERENCES

Aaron, J.E. (2012) Periosteal Sharpey's fibers: a novel bone matrix regulatory system? *Frontiers in Endocrinology*, 3, 98.
Abdala, V. & Diogo, R. (2010) Comparative anatomy, homologies and evolution of the pectoral and forelimb musculature of tetrapods with special attention to extant limbed amphibians and reptiles. *Journal of Anatomy*, 217(5), 536–573.
Bakker, R., Sullivan, R.M., Porter, V., Larson, P. & Saulsbury, S.J. (2006) *Dracorex hogwartzia*, n. gen., n. sp., a spiked, flat-headed pachycephaosaurid dinosaur from the upper cretaceous Hell Creek formation of South Dakota. In: Lucas, S.G. & Sullivan, R.M. (Eds.) *Late cretaceous vertebrate from the Western interior*. Albuquerque, NM: New Mexico Museum of Natural History and Science Bulletin, pp. 331–346.
Baron, M.G. & Williams, M.E. (2018) A re-evaluation of the enigmatic dinosauriform *Caseosaurus crosbyensis* from the late Triassic of Texas, USA and its implications for early dinosaur evolution. *Acta Palaeontologica Polonica*, 63(1), 2351.
Bell, A. & Chiappe, L.M. (2020) Anatomy of *Parahesperornis*: evolutionary mosaicism in the Cretaceous Hesperornithiformes (Aves). *Life*, 10(5), 62.
Bout, R.G. & Zweers, G.A. (2001) The role of cranial kinesis in birds. *Comparative Biochemistry and Physiology A*, 131, 197–205.
Boyd, C.A. (2014) The cranial anatomy of the neornithischian dinosaur *Thescelosaurus neglectus*. *PeerJ*, 2, e669.
Bristowe, A. & Raath, M.A. (2004) A juvenile coelophysoid skull from the early Jurassic of Zimbabwe, and the synonymy of *Coelophysis* and *Syntarsus*. *Palaeontologia Africana*, 40(40), 31–41.
Brown, B. (1916) *Corythosaurus casuarius*: skeleton, musculature and epidermis. *Bulletin of the American Museum of Natural History*, 35, 709.
Brusatte, S.L. & Carr, T.D. (2016) The phylogeny and evolutionary history of tyrannosauroid dinosaurs. *Scientific Reports*, 6(1), 20252.
Brusatte, S.L., Carr, T.D. & Norell, M.A. (2012) The osteology of *Alioramus*, a gracile and long-snouted tyrannosaurid (Dinosauria: Theropoda) from the late cretaceous of Mongolia. *Bulletin of the American Museum of Natural History*, 2012(366), 1–197.
Bryant, H.N. & Russell, A.P. (1992) The role of phylogenetic analysis in the inference of unpreserved attributes of extinct taxa. *Philosophical Transactions of the Royal Society of London. Series B: Biological Sciences*, 337(1282), 405–418.
Bryant, H.N. & Seymour, K.L. (1990) Observations and comments on the reliability of muscle reconstruction in fossil vertebrates. *Journal of Morphology*, 206(1), 109–117.
Bugos, J.E. & McDavid, S.N. (2024) Immature skulls of the theropod dinosaur *Coelophysis bauri* from ghost ranch, New Mexico. *Acta Palaeontologica Polonica*, 69(4), 549–563.
Burch, S.H. (2014) Complete forelimb myology of the basal theropod dinosaur *Tawa hallae* based on a novel robust muscle reconstruction method. *Journal of Anatomy*, 225(3), 271–297.
Butler, R.J. & Zhao, Q. (2009) The small bodied ornithischian dinosaurs *Micropachycephalosaurus hongtuyanensis* and *Wannanosaurus yansiensis* from the late cretaceous of China. *Cretaceous Research*, 2009, 63–77.
Button, D.J., Porro, L.B., Lautenschlager, S., Jones, M.E. & Barrett, P.M. (2023) Multiple pathways to herbivory underpinned deep divergences in ornithischian evolution. *Current Biology*, 33(3), 557–565.

Canale, J.I., Apesteguía, S., Gallina, P.A., Mitchell, J., Smith, N.D., Cullen, T.M. et al. (2022) New giant carnivorous dinosaur reveals convergent evolutionary trends in theropod arm reduction. *Current Biology*, 32(14), 3195–3202.

Carpenter, K. (2010) Variation in a population of Theropoda (Dinosauria): *Allosaurus* from the Cleveland-Lloyd quarry (upper Jurassic), Utah, USA. *Paleontological Research*, 14(4), 250–259.

Carr, T.D., Varricchio, D.J., Sedlmayr, J.C., Roberts, E.M. & Moore, J.R. (2017) A new tyrannosaur with evidence for anagenesis and crocodile-like facial sensory system. *Scientific Reports*, 7(1), 44942.

Chure, D.J. & Loewen, M.A. (2020) Cranial anatomy of *Allosaurus jimmadseni*, a new species from the lower part of the Morrison formation (upper Jurassic) of Western North America. *PeerJ*, 8, e7803.

Clark, J.M., Norell, M.A. & Rowe, T. (2002) Cranial anatomy of *Citipati osmolskae* (Theropoda, Oviraptorosauria), and a reinterpretation of the holotype of *Oviraptor philoceratops*. *American Museum Novitates*, 2002(3364), 1–24.

Colbert, E.H. (1970) A saurischian dinosaur from the Triassic of Brazil. *American Museum Novitates*, 24, 5651.

Currie, P.J. & Evans, D.C. (2020) Cranial anatomy of new specimens of *Saurornitholestes langstoni* (Dinosauria, Theropoda, Dromaeosauridae) from the Dinosaur Park formation (Campanian) of Alberta. *The Anatomical Record*, 303(4), 691–715.

de Buffrénil, V., Sire, J.Y. & Rage, J.C. (2010) The histological structure of glyptosaurine osteoderms (Squamata: Anguidae), and the problem of osteoderm development in squamates. *Journal of Morphology*, 271(6), 729–737.

Dempsey, M., Maidment, S.C., Hedrick, B.P. & Bates, K.T. (2023) Convergent evolution of quadrupedality in ornithischian dinosaurs was achieved through disparate forelimb muscle mechanics. *Proceedings of the Royal Society B*, 290, 20222435.

Dilkes, D.W., Hutchinson, J.R., Holliday, C.M., Witmer, L.M., Brett-Surman, M.K., Holtz, T.R. et al. (2012) Reconstructing the musculature of dinosaurs. *The Complete Dinosaur*, 20, 151–190.

Dodson, P., Forster, C.A. & Sampson, S.D. (2004) Ceratopsidae. *The Dinosauria*, 8, 494–513.

Dzik, J. (2003) A beaked herbivorous archosaur with dinosaur affinities from the early Late Triassic of Poland. *Journal of Vertebrate Paleontology*, 23(3), 556–574.

Eddy, D.R. & Clarke, J.A. (2011) New information on the cranial anatomy of Acrocanthosaurus atokensis and its implications for the phylogeny of Allosauroidea (Dinosauria: Theropoda). *PLoS One*, 6(3), e17932.

Ercoli, M.D., Álvarez, A., Warburton, N.M., Janis, C.M., Potapova, E.G., Herring, S.W. et al. (2023) Myology of the masticatory apparatus of herbivorous mammals and a novel classification for a better understanding of herbivore diversity. *Zoological Journal of the Linnean Society*, 198(4), 1106–1155.

Evans, D.C., Schott, R.K., Larson, D.W., Brown, C. & Ryan, M.J. (2013) The oldest north American pachycephalosaurid and the hidden diversity of small-bodied ornithischian dinosaurs. *Nature Communications*, 4(1828), 532.

Ezcurra, M.D. (2007) The cranial anatomy of the coelophysoid theropod *Zupaysaurus rougieri* from the upper Triassic of Argentina. *Historical Biology*, 19(2), 185–202.

Fearon, J.L. & Varricchio, D.J. (2016) Reconstruction of the forelimb musculature of the cretaceous ornithopod dinosaur *Oryctodromeus cubicularis*: implications for digging. *Journal of Vertebrate Paleontology*, 36(2), e1078341.

Ferigolo, J. & Langer, M.C. (2007) A late Triassic dinosauriform from south Brazil and the origin of the ornithischian predentary bone. *Historical Biology*, 19(1), 23–33.

Foster, W., Brusatte, S.L., Carr, T.D., Williamson, T.E., Yi, L. & Lü, J. (2021) The cranial anatomy of the long-snouted tyrannosaurid dinosaur Qianzhousaurus sinensis from the upper cretaceous of China. *Journal of Vertebrate Paleontology*, 41(4), e1999251.

Galton, P.M. (1969) The pelvic musculature of the dinosaur *Hypsilophodon* (Reptilia: Ornithischia).

Galton, P.M. & Upchurch, P. (2004) Stegosauria. In: *The Dinosauria*. Oakland, CA: University of California Press, pp. 343–362.

George, J.C. & Berger, A.J. (1966) *Avian myology*. Cambridge, MA: Academic Press.

Gignac, P.M. & Erickson, G.M. (2017) The biomechanics behind extreme osteophagy in *Tyrannosaurus rex*. *Scientific Reports*, 7(1), 2012.

Goodwin, M.B. & Evans, D.C. (2016) The early expression of squamosal horns and parietal ornamentation confirmed by new end-stage juvenile *Pachycephalosaurus* fossils from the upper cretaceous Hell Creek formation, Motana. *Journal of Vertebrate Paleontology*, 36(2), e1078343.

Grossnickle, D.M., Weaver, L.N., Jäger, K.R. & Schultz, J.A. (2022) The evolution of anteriorly directed molar occlusion in mammals. *Zoological Journal of the Linnean Society*, 194(2), 349–365.

Han, F.L., Forster, C.A., Clark, J.M. & Xu, X. (2015) Cranial anatomy of *Yinlong downsi* (Ornithischia: Ceratopsia) from the upper Jurassic Shishugou formation of Xinjiang, China. *Journal of Vertebrate Paleontology*, 36(1), e1029579.

Hassan, S.A. (2012) Comparative morphological studies on the quadratomandibular articulation in hooded crow (*Corvus cornix*) and cattle egret (*Bubulcus ibis*). *Journal of Veterinary Anatomy*, 5(1), 31–46.

Haubold, H. (1990) Ein neuer Dinosaurier (ornithischia, Thyreophora) aus dem unetren Jura des Nördlichen Mitteleuropa. *Revue de Paléobiologie*, 9(1), 149–177.

Helland, M.M. (1980) Anatomy and function of the temporomandibular joint. *Journal of Orthopaedic and Sports Physical Therapy*, 1(3), 145–152.

Herrel, A., Aerts, A. & De Vree, F. (1998) Static biting in lizards: functional morphology of the temporal ligaments. *Journal of Zoology (London)*, 244, 135–143.

Hieronymus, T.L. (2006) Quantitative microanatomy of jaw muscle attachment in extant diapsids. *Journal of Morphology*, 267(8), 954–967.

Holliday, C.M. (2009) New insights into dinosaur jaw muscle anatomy. *The Anatomical Record: Advances in Integrative Anatomy and Evolutionary Biology*, 292(9), 1246–1265.

Holliday, C.M. & Witmer, L.M. (2007) Archosaur adductor chamber evolution: integration of musculoskeletal and topological criteria in jaw muscle homology. *Journal of Morphology*, 268(6), 457–484.

Horner, H.R., Weishampel, D.B. & Forster, C.A. (2004) Hadrosauridae. In: *The Dinosauria*, 2nd edition. Oakland, CA: University of California Press, pp. 438–463.

Hu, D., Clarke, J.A., Eliason, C.M., Qiu, R., Li, Q., Shawkey, M.D. et al. (2018) A bony-crested Jurassic dinosaur with evidence of iridescent plumage highlights complexity in early paravian evolution. *Nature Communications*, 9(1), 217.

Hu, H., Wang, Y., Fabbri, M., O'Connor, J.K., McDonald, P.G., Wroe, S. et al. (2023) Cranial osteology and palaeobiology of the early cretaceous bird *Jeholornis prima* (Aves: Jeholornithiformes). *Zoological Journal of the Linnean Society*, 198(1), 93–112.

Iordansky, N.N. (1997) Jaw apparatus and feeding mechanics of *Typhlops* (Ophodia: Typhlopidae): a reconsideration. *Russian Journal of Herpetology*, 4(2), 120–127.

Iordansky, N.N. (2016) Functional relationships in the jaw apparatus of the chameleons and the evolution of adaptive complexes. *The Biological Bulletin*, 43(9), 1195–1202.

Jasinoski, S.C., Russell, A.P. & Currie, P.J. (2006) An integrative phylogenetic and extrapolatory approach to the reconstruction of dromaeosaur (Theropoda: Eumaniraptora) shoulder musculature. *Zoological Journal of the Linnean Society*, 146(3), 301–344.

Jones, S.J. & Boyde, A. (1974) The organization and gross mineralization patterns of the collagen fibres in Sharpey fibre bone. *Cell and Tissue Research*, 148, 83–96.

Kellner, A.W. (1996) Fossilized theropod soft tissue. *Nature*, 379(6560), 32.

Kirby, A., Vickaryous, M., Boyde, A., Olivo, A., Moazen, M., Bertazzo, S. et al. (2020) A comparative histological study of the osteoderms in the lizards *Heloderma suspectum* (Squamata: Helodermatidae) and *Varanus komodoensis* (Squamata: Varanidae). *Journal of Anatomy*, 236(6), 1035–1043.

Lautenschlager, S. (2013) Cranial myology and bite force performance of *Erlikosaurus andrewsi*: a novel approach for digital muscle reconstructions. *Journal of Anatomy*, 222, 260–272.

Lautenschlager, S., Gill, P., Luo, Z.X., Fagan, M.J. & Rayfield, E.J. (2017) Morphological evolution of the mammalian jaw adductor complex. *Biological Reviews*, 92(4), 1910–1940.

LeBlanc, A.R., Lamoureux, D.O. & Caldwell, M.W. (2017) Mosasaurs and snakes have a periodontal ligament: timing and extent of calcification, not tissue complexity, determines tooth attachment mode in reptiles. *Journal of Anatomy*, 231(6), 869–885.

Lee, Y.N., Barsbold, R., Currie, P.J., Kobayashi, Y., Lee, H.J., Godefroit, P. et al. (2014) Resolving the long-standing enigmas of a giant ornithomimosaur *Deinocheirus mirificus*. *Nature*, 515(7526), 257–260.

Lull, R.S. & Wright, N.E. (1942) *Hadrosaurian dinosaurs of North America*, Vol. 40. Boulder, CO: Geological Society of America.

Madsen, J.H. (1976) Allosaurus fragilis: a revised osteology.

Madzia, D., Arbour, V.M., Boyd, C.A., Farke, A.A., Cruzado-Cavallero, P. & Evans, D.C. (2021) The phylogenetic nomenclature of ornithischian dinosaurs. *PeerJ*, 9, e12362.

Mallon, J.C. & Anderson, J.S. (2014) The functional and palaeoecological implications of tooth morphology and wear for the megaherbivorous dinosaurs from the Dinosaur Park formation (upper Campanian) of Alberta, Canada. *PLoS One*, 9(6), e986905.

Mallon, J.C. & Anderson, J.S. (2015) Jaw mechanics and evolutionary paleoecology of megaherbivorous dinosaurs from the Dinosaur Park formation (upper Campanian) of Alberta, Canada. *Journal of Vertebrate Paleontology*, 35(2), 904323.

Marpmann, J.S., Carballido, J.L., Sander, P.M. & Knötschke, N. (2014) Cranial anatomy of the late Jurassic dwarf sauropod *Europasaurus holgeri* (Dinosauria, Camarasauromorpha): ontogenetic changes and size dimorphism. *Journal of Systematic Palaeontology*, 13(3), 221–263.

Maryańska, T., Chapman, R.E. & Weishampel, D.B. (2004) Pachycephalosauria. In: Weishampel, D.B., Dodson, P. & Osmólska, H. (Eds.) *The Dinosauria (2nd edition)*. Berkeley: University of California Press, pp. 464–477.

Maryańska, T. & Osmólska, H. (1974) Pachycephalosauria, a new suborder of ornithischian dinosaur. *Acta Palaeontologica Polonica*, 26, 133–182.

Maxwell, E.E. & Larsson, H.C. (2007) Osteology and myology of the wing of the emu (*Dromaius novaehollandiae*), and its bearing on the evolution of vestigial structures. *Journal of Morphology*, 268(5), 423–441.

Meinertz, T. (1944) Das superfizielle Facialisgebiet der Nager: VII. Die hystricomorphen Nager. *Zeitschrift für Anatomie und Entwicklungsgeschichte*, 113, 1–38.

Müller, R.T. & Garcia, M.S. (2020) A paraphyletic 'Silesauridae' as an alternative hypothesis for the initial radiation of ornithischian dinosaurs. *Biology Letters*, 16(8), 20200417.

Nabavizadeh, A. (2014) In: Hadrosaurs, D. & Evans, D. (Eds.) *Hadrosauroid jaw mechanics and the functional significance of the predentary bone*. Bloomington, IN: Indiana University Press.

Nabavizadeh, A. (2016) Evolutionary trends in the jaw adductor mechanics of ornithischian dinosaurs. *The Anatomical Record*, 299, 271–294.

Nabavizadeh, A. (2020a) Cranial musculature in herbivorous dinosaurs: a survey of reconstructed anatomical diversity and feeding mechanisms. *The Anatomical Record*, 303(4), 1104–1145.

Nabavizadeh, A. (2020b) New reconstruction of cranial musculature in ornithischian dinosaurs: implications for feeding mechanisms and buccal anatomy. *The Anatomical Record*, 303(2), 347–362.

Naples, V.L. (1985) Form and function of the masticatory musculature in the tree sloths, Bradypus and Choloepus. *Journal of Morphology*, 183(1), 25–50.

Nesbitt, S.J. (2009) *The early evolution of archosaurs: relationships and the origin of major clades*. New York, NY: Columbia University.

Norman, D.B. (1986) On the anatomy of *iguanodon atherfieldensis* (Ornithischia: Ornithopoda). *Bulletin-Institut royal des sciences naturelles de Belgique. Sciences de la Terre*, 56, 281–372.

Norman, D.B. (2004) Basal Iguanodontia. *The Dinosauria*, 2, 413–437.

Norman, D.B. (2020) *Scelidosaurus harrisonii* from the early Jurassic of Dorset, England: cranial anatomy. *Zoological Journal of the Linnean Society*, 188(1), 1–81.

Novas, F.E., Agnolin, F.L., Ezcurra, M.D., Müller, R.T., Martinelli, A.G. & Langer, M.C. (2021) Review of the fossil record of early dinosaurs from South America, and its phylogenetic implications. *Journal of South American Earth Sciences*, 110, 103341.

Osborn, J.W. (1989) The temporomandibular ligament and the articular eminence as constraints during jaw opening. *Journal of Oral Rehabilitation*, 16(4), 323–333.

Pacheco, C., Müller, R.T., Langer, M., Pretto, F.A., Kerber, L. & da Silva, S.D. (2019a) *Gnathovorax cabreirai*: a new early dinosaur and the origin and initial radiation of predatory dinosaurs. *PeerJ*, 7, e7963.

Pacheco, C., Müller, R.T., Langer, M.C., Pretto, F., Kerber, L. & da Silva, S.D. (2019b) 3D models related to the publication: *Gnathovorax cabreirai*: a new early dinosaur and the origin and initial radiation of predatory dinosaurs. *MorphoMuseuM*, 5, e103.

Pei, R., Li, Q., Meng, Q., Norell, M.A. & Gao, K.Q. (2017) New specimens of *Anchiornis huxleyi* (Theropoda: Paraves) from the late Jurassic of northeastern China. *Bulletin of the American Museum of Natural History*, 2017(411), 1–67.

Pereira, F.M.A.M., Bete, S.B.D.S., Inamassu, L.R., Mamprim, M.J. & Schimming, B.C. (2020) Anatomy of the skull in the capybara (*Hydrochoerus hydrochaeris*) using radiography and 3D computed tomography. *Anatomia, Histologia, Embryologia*, 49(3), 317–324.

Perle, A., Maryańska, T. & Osmólska, H. (1982) *Goyocephale lattimorei* gen. Et sp. n., a new flat-headed pachycephalosaur (Ornithischia, Dinosauria) from the upper cretaceous of Mongolia. *Acta Palaeontologica Polonica*, 27(1–4), 115–127.

Petermann, H. & Sander, M. (2013) Histological evidence for muscle insertion in extant amniote femora: implications for muscle reconstruction in fossils. *Journal of Anatomy*, 222(4), 419–436.

Rauhut, O.W., Milner, A.C. & Moore-Fay, S. (2010) Cranial osteology and phylogenetic position of the theropod dinosaur *Proceratosaurus bradleyi* (Woodward, 1910) from the middle Jurassic of England. *Zoological Journal of the Linnean Society*, 158(1), 155–195.

Romer, A.S. (1923) Crocodilian pelvic muscles and their avian and reptilian homologues. *Bulletin of the AMNH*, 48, 15.

Rowe, T. (1986) Homology and evolution of the deep dorsal thigh musculature in birds and other Reptilia. *Journal of Morphology*, 189(3), 327–346.

Rowe, T. (1989) A new species of the theropod dinosaur *Syntarsus* from the early Jurassic Kayenta formation of Arizona. *Journal of Vertebrate Paleontology*, 9(2), 125–136.

Saber, A.S.M. & Hassanin, A. (2014) Some morphological studies on the jaw joint of the australian saltwater crocodile (*Crocodylus porosus*). *Journal of Veterinary Anatomy*, 7(2), 55–74.

Sampson, S.D. & Witmer, L.M. (2007) Craniofacial anatomy of *Majungasaurus crenatissimus* (Theropoda: Abelisauridae) from the late cretaceous of Madagascar. *Journal of Vertebrate Paleontology*, 27(S2), 32–104.

Scheetz, R.D. (1999) *Osteology of Orodromeus makelai and the phylogeny of basal ornithopod dinosaurs*. Bozeman, MT: Montana State University.

Scheyer, T.M., Sander, P.M., Joyce, W.G., Böhme, W. & Witzel, U. (2007) A plywood structure in the shell of fossil and living soft-shelled turtles (Trionychidae) and its evolutionary implications. *Organisms Diversity & Evolution*, 7(2), 136–144.

Sena, M.V.D.A., Marinho, T.D.S., Montefeltro, F.C., Langer, M.C., Fachini, T.S., Nava, W.R. et al. (2023) Osteohistological characterization of

notosuchian osteoderms: evidence for an overlying thick leathery layer of skin. *Journal of Morphology*, 284(1), e21536.
Sereno, P.C. (2012) Taxonomy, morphology, masticatory function and phylogeny of heterodontosaurid dinosaurs. *ZooKeys*, 226, 1–562.
Sereno, P.C., Dutheil, D.B., Iarochene, M., Larsson, H.C., Lyon, G.H., Magwene, P.M. et al. (1996) Predatory dinosaurs from the Sahara and late cretaceous faunal differentiation. *Science*, 272(5264), 986–991.
Sereno, P.C., Martínez, R.N. & Alcober, O.A. (2012) Osteology of *Eoraptor lunensis* (Dinosauria, sauropodomorpha). *Journal of Vertebrate Paleontology*, 32(sup1), 83–179.
Sereno, P.C. & Novas, F.E. (1994) The skull and neck of the basal theropod *Herrerasaurus ischigualastensis*. *Journal of Vertebrate Paleontology*, 13(4), 451–476.
Sereno, P.C., Xijin, Z. & Lin, T. (2010) A new psittacosaur from Inner Mongolia and the parrot-like structure and function of the psittacosaur skull. *Proceedings of the Royal Society B: Biological Sciences*, 277(1679), 199–209.
Sharpey, W. & Schäfer, E.A. (1878) Notes on the structure and development of osseous tissue. *Journal of Cell Science*, 2(70), 132–144.
Sharpey, W., Thompson, A. & Cleland, J. (1867) *Quain's elements of anatomy*, 7th edition. London: James Walton.
Simmons, D.J., Menton, D.N., Miller, S. & Lozano, R. (1993) Periosteal attachment fibers in the rat calvarium. *Calcified Tissue International*, 53, 424–427.
Skedros, J.G., Mendenhall, S.D., Kiser, C.J. & Winet, H. (2009) Interpreting cortical bone adaptation and load history by quantifying osteon morphotypes in circularly polarized light images. *Bone*, 44(3), 392–403.
Snively, E. & Russell, A.P. (2007) Craniocervical feeding dynamics of *Tyrannosaurus rex*. *Paleobiology*, 33(4), 610–638.
Sues, H.-D. & Galton, P. (1987) Anatomy and classification of the north American Pachycephalosauria (Dinosauria: Ornithischia). *Palaeontographica Abteilung A*, 198(1–3), 1–40.
Sues, H.D., Nesbitt, S.J., Berman, D.S. & Henrici, A.C. (2011) A late-surviving basal theropod dinosaur from the latest Triassic of North America. *Proceedings of the Royal Society B: Biological Sciences*, 278(1723), 3459–3464.
Sullivan, C. & Xu, X. (2017) Morphological diversity and evolution of the jugal in dinosaurs. *The Anatomical Record*, 300(1), 30–48.
Taylor, A.C., Lautenschlager, S., Qi, Z. & Rayfield, E.J. (2017) Biomechanical evaluation of different musculoskeletal arrangements in *Psittacosaurus* and implications for cranial function. *The Anatomical Record*, 300(1), 49–61.
Tokita, M. (2004) Morphogenesis of parrot jaw muscles: understanding the development of an evolutionary novelty. *Journal of Morphology*, 259(1), 69–81.
Tsogtbaatar, K., Weishampel, D.B., Evans, D.C. & Watabe, M. (2019) A new hadrosauroid (Dinosauria: Ornithopoda) from the late cretaceous Baynshire formation of the Gobi Desert (Mongolia). *PLoS One*, 14(4), e0208480.
Varriale, F.J. (2016) Dental microwear reveals mammal-like chewing in the neoceratopsiand dinosaur *Leptoceratops gracilis*. *PeerJ*, 4, 2132.
Venkatesan, S., Nizzar, S., Basha, S.H., Kannan, T.A. & Ramesh, G. (2015) Morphology of jaw ligaments and its role in the cranial kinesis of the domestic Turkey (*Meleagris gallopavo*). *Journal of Veterinary Anatomy*, 27(2), 45–47.
Vickaryous, M.K. (2006) New information on the cranial anatomy of *Edmontonia rugosidens* Gilmore, a late cretaceous nodosaurid dinosaur from dinosaur Provincial Park, Alberta. *Journal of Vertebrate Paleontology*, 26(4), 1011–1013.
Vickaryous, M.K., Maryanska, T. & Weishampel, D.B. (2004) Ankylosauria. In: *The Dinosauria*, Second edition. Berkeley, CA: University of California Press, pp. 363–392.
Wang, M. & Hu, H. (2017) A comparative morphological study of the jugal and quadratojugal in early birds and their dinosaurian relatives. *The Anatomical Record*, 300(1), 62–75.
Wang, M., Stidham, T.A., Li, Z., Xu, X. & Zhou, Z. (2021) Cretaceous bird with dinosaur skull sheds light on avian cranial evolution. *Nature Communications*, 12(1), 3890.
Weishampel, D.B., Dodson, P. & Osmólska, H. (Eds.). (2004) *The Dinosauria*. Oakland, CA: University of California Press.
Weishampel, D.B., Jianu, C.M., Csiki, Z. & Norman, D.B. (2003) Osteology and phylogeny of *Zalmoxes* (ng), an unusual euornithopod dinosaur from the latest cretaceous of Romania. *Journal of Systematic Palaeontology*, 1(2), 65–123.
Wellnhofer, P. (2009) *Archaeopteryx: The Icon of Evolution*. Munich: Dr. Friedrich Pfeil Verlag.
Whitebone, S.A., Bari, A.H., Gavrilova, M.L. & Anderson, J.S. (2021) A multimethod approach to the differentiation of enthesis bone microstructure based on soft tissue type. *Journal of Morphology*, 282(9), 1362–1373.
Wilson, J.A. & Sereno, P.C. (1998) Early evolution and higher-level phylogeny of sauropod dinosaurs. *Journal of Vertebrate Paleontology*, 18(S2), 1–79.
Wilson, J.A., Pol, D., Carvalho, A.B. & Zaher, H. (2016) The skull of the titanosaur *Tapuiasaurus macedoi* (Dinosauria: Sauropoda), a basal titanosaur from the Lower Cretaceous of Brazil. *Zoological Journal of the Linnean Society*, 178(3), 611–662.
Witmer, L.M. (1995) The extant phylogenetic bracket and the importance of reconstructing soft tissues in fossils. *Functional Morphology in Vertebrate Paleontology*, 1, 19–33.
Wu, W.H., Godefroit, P. & Hu, D. (2010) *Bolong yixianensis* gen. Et sp. nov.: a new iguanodontoid dinosaur from the Yixian formation of western Liaoning, China. *Geology and Resources*, 19(2), 127–133.
Xu, X., Wang, K., Zhang, K., Ma, Qingyu., Xing, L., Sullivan, C. et al. (2012) A gigantic feathered dinosaur from the lower cretaceous of China. *Nature (London)*, 484(7392), 92–95.
Zaher, H., Pol, D., Carvalho, A.B., Nascimento, P.M., Riccomini, C., Larson, P. et al. (2011) A complete skull of an early cretaceous sauropod and the evolution of advanced titanosaurians. *PLoS One*, 6(2), e16663.
Zheng, X., Bailleul, A.M., Li, Z., Wang, X. & Zhou, Z. (2021) Nuclear preservation in the cartilage of the Jehol dinosaur *Caudipteryx*. *Communications Biology*, 4(1), 1125.
Zusi, R.L. (1993) Patterns of diversity in the avian skull. *The Skull*, 2, 391–437.
Zhou, Z., Zhang, F. & Li, Z. (2009) A new basal ornithurine bird (*Jianchangornis microdonta* gen. et sp. nov.) from the Lower Cretaceous of China. *Vertebrata PalAsiatica*, 47, 299–310.
Zhou, Z., Clarke, J. & Zhang, F. (2008) Insight into diversity, body size and morphological evolution from the largest Early Cretaceous enantiornithine bird. *Journal of Anatomy*, 212(5), 565–577.
Zhou, S., Zhou, Z. & O'Connor, J.K. (2013) Anatomy of the basal ornithuromorph bird *Archaeorhynchus spathula* from the Early Cretaceous of Liaoning, China. *Journal of Vertebrate Paleontology*, 33(1), 141–152.

SUPPORTING INFORMATION

Additional supporting information can be found online in the Supporting Information section at the end of this article.

How to cite this article: Sharpe, H.S., Wang, Y.-y., Dudgeon, T.W., Powers, M.J., Whitebone, S.A., Coppock, C.C. et al. (2025) Skull morphology and histology indicate the presence of an unexpected buccal soft tissue structure in dinosaurs. *Journal of Anatomy*, 00, 1–29. Available from: https://doi.org/10.1111/joa.14242